THERMODYNAMIC AND EXERGO-ECONOMIC ANALYSIS OF A COMBINED POWER PLANT ON GAS TURBINE CYCLE AND ORGANIC RANKINE CYCLE

2023
MASTER THESIS
MECHANICAL ENGINEERING

Alaa Fadhil KAREEM

Thesis Advisor
Assist. Prof. Dr. Abdulrazzak AKROOT

THERMODYNAMIC AND EXERGO-ECONOMIC ANALYSIS OF A COMBINED POWER PLANT ON GAS TURBINE CYCLE AND ORGANIC RANKINE CYCLE

Alaa Fadhil KAREEM

Thesis Advisor
Assist. Prof. Dr. Abdulrazzak AKROOT

T.C.
Karabük University
Institute of Graduate Programs
Department of Mechanical Engineering

Prepared as
Master Thesis

KARABÜK
January 2023

I certify, that in my opinion, the thesis submitted by Alaa Fadhil Kareem titled "THERMODYNAMIC AND EXERGO-ECONOMIC ANALYSIS OF A COMBINED POWER PLANT ON GAS TURBINE CYCLE AND ORGANIC RANKINE CYCLE" is fully adequate in scope and in quality as a thesis for the degree of Master of Science.

Assist. Prof. Dr. Abdulrazzak AKROOT .....
Thesis Advisor, Department of Mechanical Engineering

This thesis is accepted by the examining committee with a unanimous vote in the Department of Mechanical Engineering as a Master of Science thesis. …/01/2023

Examining Committee Members (Institutions)	Signature
Chairman : Prof. Dr. Yaşar YETİŞKEN (KBU)	.....
Member: Assoc. Prof. Dr. Lütfü NAMLI (OMU)	.....
Member: Assist. Prof. Dr. Abdulrazzak AKROOT (KBU)	.....

The degree of Master of Science by the thesis submitted is approved by the Administrative Board of the Institute of Graduate Programs, Karabük University.

Prof. Dr. Müslüm KUZU .....
Director of the Institute of Graduate Programs

This thesis contains information that I have gathered and presented in a manner that is consistent with academic regulations and ethical principles, and I affirm that I have appropriately cited any and all sources that are not my own work.

Alaa Fadhil KAREEM

ABSTRACT

M. Sc. Thesis

THERMODYNAMIC AND EXERGO-ECONOMIC ANALYSIS OF A COMBINED POWER PLANT ON GAS TURBINE CYCLE AND ORGANIC RANKINE CYCLE

Alaa Fadhil KAREEM

Karabük University
Institute of Graduate Programs
The Department of Mechanical Engineering

Thesis Advisor:
Assist. Prof. Dr. Abdulrazzak AKROOT
January 2023, 68 pages

Organic Rankine cycles (ORCs) are a suitable approach to transform low-quality thermal energy into electricity. Additionally, the release of waste heat to the atmosphere from the exhaust gases produced during the top cycle of the energy conversion systems is avoided. The main objective of this work is to integrate the Taji gas station, which is in Baghdad, with the Rankine cycle and organic Rankine cycle to verify waste heat recovery to produce extra electricity and reduce emissions into the environment. Thermodynamic and exergo-economic assessment of the combined Brayton cycle-Rankine cycle/Organic Rankin cycle (GSO CC) system, considering the three objective functions of First and Second Law efficiencies and the total cost rates of the system, were applied. According to the findings, 258.2 MW of power is produced from the GSO CC system, whereas 167.3 MW of power is created for the Brayton cycle (BC) at the optimum operating condition. It was demonstrated that the

overall energy and exergy efficiencies respectively are 44.37% and 42.87% for the GSO CC system, while they are 28.74% and 27.75% respectively for the Brayton cycle. Moreover, the GSO CC system is $9.03/MWh, whereas it is $8.24/MWh for BC. The results also indicate that the network of the GSO CC system decreases as the pressure ratio increases. Nonetheless, the GSO CC system's efficiencies and costs increase with a rise in the pressure ratio until they reach a maximum and then decrease with further pressure ratio increases. The increase in the gas turbine inlet temperature and isentropic efficiency of the air compressor and gas turbine enhances the thermodynamic performance of the system; however, a further increase in these parameters increases the overall cost rates.

Keywords **:** Exergo-economic analysis, Cost rate, Thermodynamic combined cycle, organic Rankine cycle.

Science Code : 91436

ÖZET

Yüksek Lisans Tezi

KOMBİNE BİR ELEKTRİK SANTRALİNİN GAZ TÜRBİNİ ÇEVRİMİ VE ORGANİK RANKİNE ÇEVRİMİ ÜZERİNDE TERMODİNAMİK VE EXERGO-EKONOMİK ANALİZİ

Ala Fadhil KAREEM

Karabük Üniversitesi
Lisansüstü Eğitim Enstitüsü
Makine Mühendisliği Bölümü

Tez Danışmanı:
Dr. Öğr. Üyesi Abdulrazzak AKROOT
Ocak 2023, 68 sayfa

Organik Rankine çevrimleri (ORC'ler), düşük kaliteli termal enerjiyi elektriğe dönüştürmek için uygun bir yaklaşımdır. Ayrıca, enerji dönüşüm sistemlerinin en üst çevrimi sırasında oluşan egzoz gazlarının atık ısısının atmosfere salınması engellenir. Bu çalışmanın temel amacı, fazladan elektrik üretmek ve çevresel emisyonları azaltmak için atık ısı geri kazanımını doğrulamak için Bağdat'ta bulunan Taji benzin istasyonunu Rankine çevrimi ve organik Rankine çevrimi ile entegre etmektir. Kombine Brayton çevrimi-Rankine çevrimi / Organik Rankin çevrimi (GSO CC) sisteminin termodinamiği ve eksergo-ekonomik değerlendirmesi, birinci ve ikinci yasa verimliliklerinin üç amaç fonksiyonu ve sistemin toplam maliyet oranları dikkate alınarak uygulanmıştır. Elde edilen bulgulara göre GSO CC sisteminden 258,2 MW güç üretilirken optimum çalışma koşulunda Brayton çevrimi (BC) için 167,3 MW güç üretiliyor. Toplam enerji ve ekserji verimlerinin GSO CC sistemi için %44,37 ve

%42,87 olduğu, Brayton çevrimi için ise %28,74 ve %27,75 olduğu gösterilmiştir. Ayrıca GSO CC sistemi 9,03 $/MWh iken BC için 8,24 USD/MWh'dir. Sonuçlar ayrıca GSO CC sisteminin iş ağının basınç oranı arttıkça azaldığını da göstermektedir. Bununla birlikte, GSO CC sisteminin verimlilikleri ve maliyetleri, maksimuma ulaşana kadar basınç oranındaki artışla artar ve daha sonra basınç oranı arttıkça azalır. Hava kompresörü ve gaz türbininin gaz türbini giriş sıcaklığındaki ve izantropik verimliliğindeki artış, sistemin termodinamik performansını artırır; bununla birlikte, bu parametrelerdeki daha fazla artış, toplam maliyet oranlarını artırır.

Anahtar Kelimeler : Eksergo-ekonomik analiz, Maliyet oranı, Termodinamik kombine çevrim, organik Rankine çevrimi.

Bilim Kodu **:** 91436

ACKNOWLEDGEMENT

O Allah, benefit me with what you have taught me, and teach me what will benefit me, and increase my knowledge. Praise be to God, with Whose grace good deeds are accomplished, and thanks to Whom blessings perpetuate. And prayers and peace be upon the best of creation, our Prophet Muhammad and his good and pure family and companions, I dedicate this humble effort to those who have led me from the beginning to the shore of success, to those who raised me when I was young, encouraged me, raised my status, supported me in their prayers and supplications, and did not hold anything back for the sake of my comfort and success, and taught me that the world is a struggle and its weapon is science and knowledge to my sun and moon, my dear father and dear mother, those who, no matter what I do and write, do not fulfill their right, you are the light of my path.

To those whom I had in this world, my brothers Muhammad and Ali, and my sister Aseel Mays, my little sister, who supported me and accompanied me throughout the study period and gave everything she could to complete this work.

To my Teacher and Teachers, Assist. Prof. Dr. Abdulrazzak AKROOT, who was credited with teaching me, providing advice and guidance, and expressing his opinion throughout the study period, and who has been the best reference for me. I also thank the Head of the Department of Mechanical Engineering, Prof. Dr. Kamil ARSLAN and his staff.

To everyone who supported me and extended a helping hand, especially Dr. Taha Malik Mansoor and Engineer Omar Adnan Hamad, I wish them success. I also dedicate this achievement to my dear country, Iraq, and my beloved city, Baghdad, steadfast in its people, and to the country that hosted me throughout my study period, Turkey.

CONTENTS

Page

Page

LIST OF FIGURES

Page

LIST OF TABLES

Page

SYMBOLS AND ABBREVITIONS INDEX

SYMBOL

$\dot{m}_{in}$: Total mass flow entering per unit of time

$\dot{m}_{out}$: Total mass flow exiting per unit time

$\dot{Q}$: Heat transfer per unit time

$\dot{W}$: Work done by the control volume per unit time

h_{in} : Specific enthalpy per mass entering the system

h_{out} : Specific enthalpy per mass leaving the system

s_0 : Specific entropy of mass entering the open system

s : Specific entropy of mass emanating from the open system

T_0 : Boundary temperature between the open system and the environment

$\dot{E}$: Exergy flows

ψ : Specific exergy

$\dot{E}_{P,AC}$: Product exergy for the compressor

$\dot{E}_{f,AC}$: Fuel exergy for the compressor

ε_{AC} : Exergy efficiency exergy for the compressor

PEC : Equipment purchase cost in US dollars

φ : Maintenance factor (1.06)

CRF : Capital Recovery Factor

i : Interest rate (considered to be 10%)

n : System lifetime (considered to be 20 years)

C : is the cost rate ($/h)

$\dot{Z}_k$: represents the entire cost rate related to capital investment and operation and maintenance costs component k

ABBREVITIONS

BC	: Brayton cycle
RC	: Rankine cycle
ORC	: Organic Rankine cycle
GSO CC	: Gas steam Organic combined cycle
GT	: Gas turbine
CC	: Combustion chamber
AC	: Air compressor
P	: Pump
CON	: Condenser
ST	: Steam turbine
HRSG	: Heat recovery steam generation
HE	: Heat exchanger
ORT	: Organic Rankine turbine
HRB	: Heat recovery boiler
GTIT	: Gas turbine inlet temperature
EES	: Engineering Equation Solver

PART 1

INTRODUCTION

1.1. GENERAL

Energy has become a critical need from which people benefit in their daily lives. This makes the trend toward energy production more attractive. Many sources, such as wind, solar, tidal, fossil, and nuclear energy, are used in energy production. For developing countries, the energy obtained by fossil fuels maintains its importance and is increasingly coming to the fore. This trend increases investments in energy production facilities using fossil fuels. A combined cycle power plant (CCPP) is one type of energy production facility in existence around the world and in our country in which fossil fuels are used. Many current studies aim to reduce production costs and maximize energy outputs in response to the rising demand for energy. Therefore, there have been enhancements to the technology used to provide energy. There has been a notable shift in recent years toward using renewable energy sources and power plants with a smaller carbon footprint and less impact on the planet's climate. Thermodynamic analysis, used to identify inefficiencies, and followed by the creation of practical alternatives, is the most efficient method for the reduction of energy losses in a system. In line with the results obtained by conducting energy and exergy analyses, it is emphasized that the improvements to increase the thermal efficiency of power plants can be evaluated more effectively. In addition, energy and exergy analyses are applied together in studies on understanding the effects of changing environmental conditions on the thermal efficiency of thermal power plants and optimizing plant designs according to environmental conditions or the selection of a location. In some of these studies, modeling and simulation applications were used employing computer software in thermodynamic analysis. By running the same thermodynamic analyses several times at varied values for variables such as thermal power plant operating load,

outside temperature, outdoor air pressure, outdoor relative humidity, and cooling water temperature, it is now simpler to identify the impacts on thermal efficiency.

The Taji gas station was established to produce electric power in 1976 in Baghdad. It operates on liquid and gaseous fuels and consists of seven generating units. The designed energy production per unit is 25 megawatts. In 2012, four new generating units were added, each producing 40 megawatts.

Thermal efficiency between 30% and 40% can be obtained using only the gas turbine. However, in addition to the Brayton cycle, steam can be produced in the waste heat recovery generation and generated in the Rankine cycle. By using only waste heat without burning extra fuel, the thermal efficiency level can be increased between 50% and 60% with the help of newly developed technologies. Power plants that generate power in this manner are called combined cycle power plants.

1.2. PROBLEM STATEMENT

Energy is now the primary driver of nation-building, industrialization, and the expansion of developed nations through increasing production. Because nations' desires for development and empowerment are growing, so too is their need for energy to a significant extent. The world's energy needs are currently being met using fossil fuels. It is crucial to ensure that these fuels are used effectively and efficiently while the search for alternate energy sources intensifies. In addition, there has been a rise in the preference for renewable energy sources versus depleting sources for environmental and economic reasons. Using fossil fuels increases environmental dangers, such as excessive carbon dioxide emissions and global warming. For these reasons, research is being conducted to improve the efficiency of current production systems or use more renewable resources to produce energy. Waste heat recovery methods are one way to use already available resources better.

Energy conservation is the practice of producing and using energy as efficiently as possible, eliminating energy losses, identifying the energy requirements that will not impede economic development and quality of life, and halting or limiting the growth

in energy consumption. The industry examines energy efficiency and savings in various ways, and energy analysis improves system performance. By looking at the system thermos-economically, it is intended to lower energy costs and boost energy efficiency in this context. The primary power generation system can be integrated with other systems to recover significant waste heat. Systems that generate power simultaneously can produce more electricity. Through this research, we hope to create a Rankine cycle and an organic Rankine cycle (ORC) and combine them with the Taji gas station in Baghdad to recover waste heat, produce additional electricity and reduce environmental emissions.

Iraq suffers from a major shortage of electrical power which causes significant losses to the national economy and disrupts the wheel of reconstruction and progress. The lack of a reliable power source from the grid has also led to the widespread installation of private diesel generators, the continuous operation of which imposes high costs, and creates noise and air pollution as they release large amounts of carbon into the atmosphere. It is estimated that the losses in the Iraqi economy attributable to this energy shortage exceed $40 billion annually.

Therefore, alternative solutions must be found to increase the production of electricity. One of these solutions is the subject of our research: to take advantage of exhaust gas heat, as the lost heat from turbine exhausts is recovered to generate steam. The steam from the waste heat is forced through a steam turbine to provide additional electricity and to reduce pollution from exhaust emissions.

1.3. THERMAL POWER PLANT

The term “thermal power cycle plant” refers to systems that may produce heat and electricity from a single engine in several forms using only one fuel input. CHP is also known as a cogeneration system or a combined heat and power system. Although natural gas is typically the fuel input, other options include fuel oil, biogas, and biofuel [1]. Today, thermal power plant systems are extensively employed. Both generate electricity from fuel inputs and boost system efficiency by producing steam and hot water while somewhat lowering the cost of the facility’s energy requirements.

When a combined system power plant is used, the losses in the system result from the conversion of the waste heat of the gas engine to the system's reusable energy. Thus, the system functions more effectively and is given energy efficiency [2].

CHP is a high-tech system that uses the waste heat generated by the fuel utilized with the gas engine. The efficiency of the cycle as a whole is improved, particularly for CO_2, and greenhouse gas emissions are significantly reduced [3]. Thermal power cycle plants create steam and hot water by converting the exhaust heat from the system into usable energy. In conclusion, it enables the creation of several heat and electricity sources using a single system. Additionally, the thermal efficiency of the system is boosted by limiting the direct emission of waste heat from the system through exhaust after power generation and ensuring that the waste heat is evaluated. Gas-engine thermal power-cycle power plants are both more effective in terms of efficiency and more sophisticated in terms of system technology than thermal power plants that generate electricity using natural gas [4]. The production of steam and hot water using the waste heat energy released after electrical energy is generated is the most distinguishing characteristic of the gas engine thermal power conversion plant compared to traditional power plants. Gas turbine and waste heat recovery systems are the two main categories under which combined power system components are often categorized [5].

1.3.1. Gas Turbine Thermal Power Cycle Plant

The Brayton cycle, developed by George Brayton around 1870, is used in motors that run on reciprocating oil [6]. It is now only practical for gas turbines, which perform compression and expansion using spinning machinery [7]. As shown in Figure 1.1, combustion is achieved in gas turbine thermal power cycle facilities by combining compressed air and fuel through the compressor. The turbine section receives the energy from combustion and transfers it to the shaft to cause the shaft to rotate mechanically and produce electricity [8].

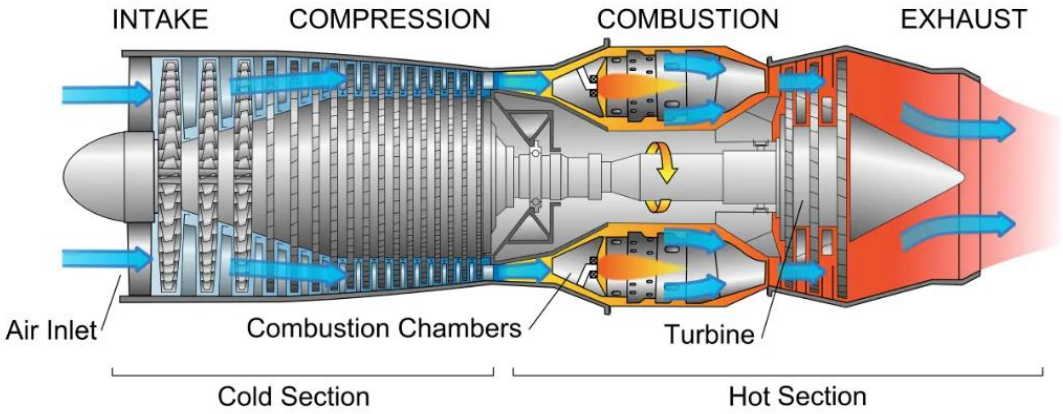

Figure 1.1. Gas Turbine System [8].

Gas turbines, as depicted above, typically operate in what is called an open cycle. Atmospheric air is sucked into the compressor, which is heated and compressed. The fuel is continuously burned in a chamber where high-pressure air is injected [9]. The expanded, high-temperature gases next enter the turbine, where their pressure is reduced to that of the surrounding air. It is considered an open cycle since the turbine exhaust is released into the atmosphere rather than recycled. A closed cycle is an alternative way of seeing the open gas turbine cycle described above. Gas turbines rely heavily on natural gas as a fuel source [10]. Other options include biogas, kerosene, distillates, LPG, and liquid fuels. System configurations utilizing gas turbines often operate at very high temperatures and velocities. This necessitates the highest-grade fuel available. Particularly, the particles in the combustion gases that can erode the turbine blades must be eliminated. Moreover, corrosion-causing impurities should be kept below a threshold [11].

1.3.2. Waste Heat Recovery Systems

The simplest definition of waste heat is the thermal energy that develops after a process and leaves the system unutilized. According to the rules of thermodynamics, waste heat is produced in every operation that has thermodynamic cycles. When assessing waste heat, quality matters more than quantity. Waste heat recovery methods are selected in accordance with these temperature values since waste heat quality is temperature-dependent [12]. Almost any temperature which varies depending on the

process type can release waste heat into the environment. High waste heat temperatures typically indicate better quality and more effective heat recovery [13].

Thermodynamic cycles are typically seen in systems created for energy recovery from exhaust gases. In its most basic form, a thermodynamic cycle for heat recovery consists of two heat exchangers, one acting as an evaporator and the other as a condenser, a pump for pressure increase and circulation, a turbine for mechanical power generation and expansion to the low-pressure stage, and a working fluid that transfers energy. With waste heat recovery systems, the efficiency of the gas power cycle has significantly increased [14,15].

1.4. RANKINE CYCLE

The Rankine cycle, or the Rankine steam cycle, is the most widely used cycle in power production plants such as nuclear reactor plants or power plants that use coal in their work, where fuel is used to produce great heat inside a boiler in which water is converted into steam. The steam expands inside turbines to produce useful work. This process was developed by the Scottish engineer William J.M. Rankin in 1859 [16]. This is considered a thermodynamic cycle, where heat is converted into mechanical and electrical energy by generating electricity.

The steps of the Rankine cycle are explained in Figure 1.2 and in Figure 1.3 on the volume-pressure diagram [17,18].

- Pump: The pumped liquid pressure is increased (this takes work) (Figure 1.3: Steps 3 and 4).
- Boiler: The pressurized liquid is converted by heating to the final temperature at the boiling point (Figure 1.3: Steps 4 to 1).
- Turbine: Pressure is reduced by an expansion process that occurs in the turbine. This results in work (Figure 1.3: Steps 1 and 2).
- Condenser: In the condenser, the process of condensing steam takes place, and the heat from condensation goes into the atmosphere (Figure 1.3: Steps 2 and 3).

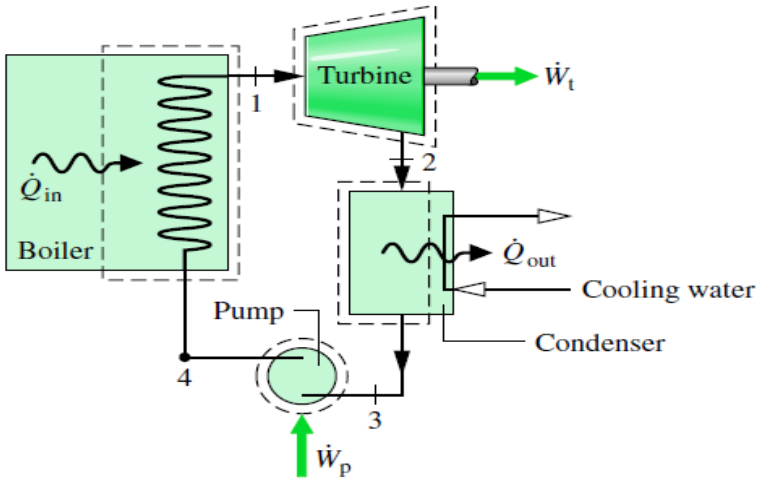

Figure 1.2. A simple schematic drawing of the components of the Rankine cycle [19].

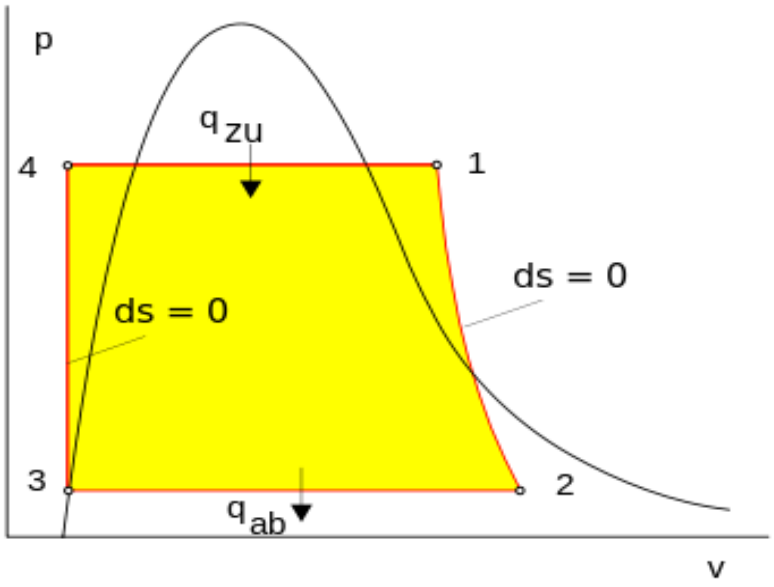

Figure 1.3. Volume-pressure diagram for a Rankine cycle using water as the working fluid [19].

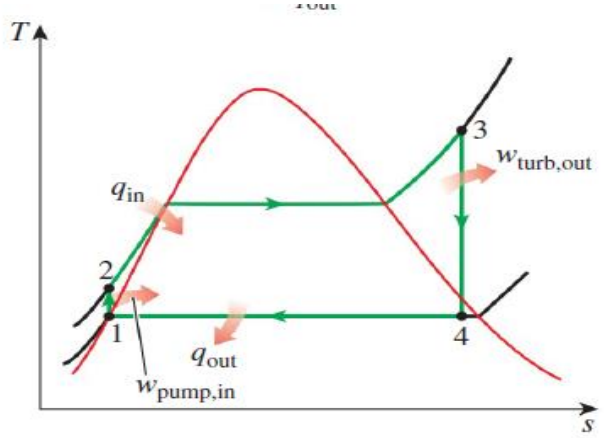

Figure 1.4. Temperature-entropy diagram for a Rankine cycle [18].

Because of the high heat of evaporation, the efficiency of the Rankine cycle is limited, so the liquid must be reused, i.e., recycled continuously. Therefore, water is the most used liquid in this cycle. This is what makes us find many energy-producing stations near water bodies because of the waste heat.

In the condenser, water is condensed and turned into water vapor, and in the process, waste heat is emitted .This steam flows from the station's cooling towers and can be seen as it flows from the cooling towers .This waste heat is essential to any thermodynamic cycle. As a result of condensation, the pressure is low at the outlet of the turbine, which reduces the work required for the pump's water pressure, increasing the cycle's overall efficiency [19].

1.5. BRAYTON CYCLE

The Brayton cycle is a thermodynamic cycle used for gas turbines and jet engines. The cycle begins with the pressure of the surrounding air; then, the fuel is mixed with the air, after which the mixture is ignited. This mixture expands and does the necessary work. The efficiency of the Brayton cycle can be increased by circulating hot air. In turn, the fresh air coming through it is heated, i.e., the amount of fuel required to heat the fresh air is reduced, which increases the efficiency of the cycle. In physics terms, the Brayton cycle is of constant pressure and expands when heating and cooling are equal to pressure, and the efficiency of other cycles can be increased [20].

Some attempts have been made to change the idea of the Brayton cycle in the designs of nuclear power plants by using hot gas from the reactor core to operate the turbine, as in the example of the standard Pebble-Bed reactor [21]. Despite research and significant development, this is still difficult and unsuccessful in South Africa in certain molten salt reactors. A steam engine is used in the nuclear reactors that operate in the Rankine cycle instead, and this necessitates that we adopt the current models, which are cooled by gas, using this heated gas to heat the water for the steam engine turbines [22].

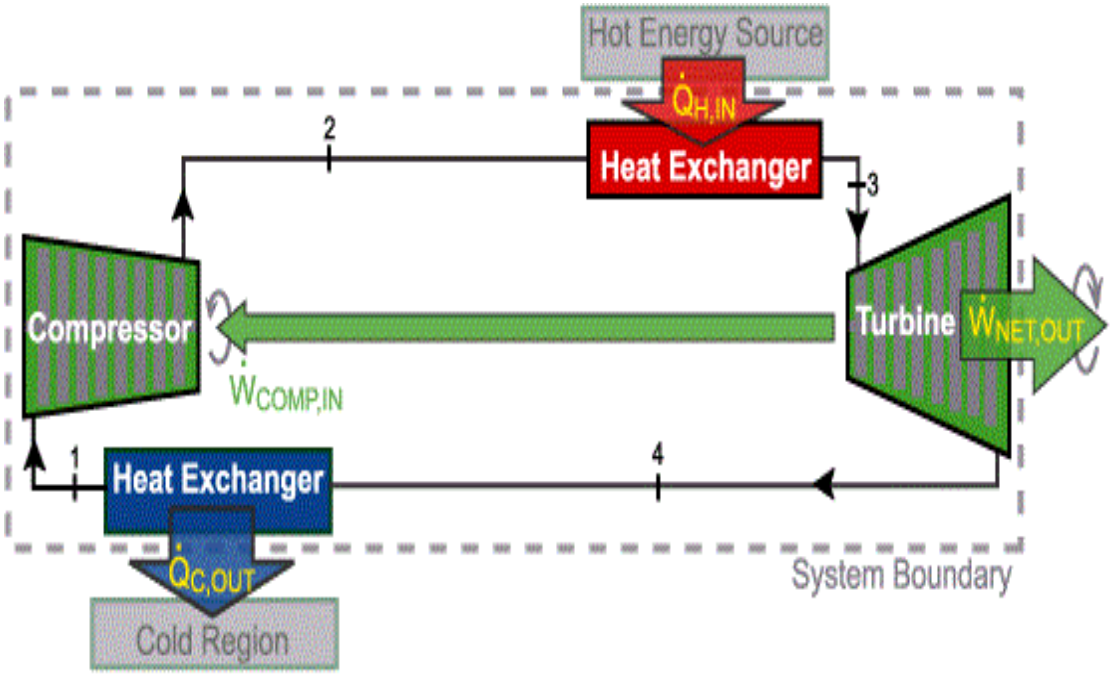

Figure 1.5. Reheat and regeneration in the Brayton cycle [23].

1.6. ORGANIC RANKINE CYCLE

It is known that the Organic Rankine cycle uses an organic liquid. In contrast, water is used as the working fluid of the organic liquid and has a high molecular mass as its principle of operation. It is similar to the work of the classic Rankine cycle, which consists of a pump pumping the working fluid to the boiler where it evaporates [24]. Then it proceeds through an expanding device (turbine) and finally goes into a heat exchanger (condenser) in which it is recycled as condensation of the working fluid, as seen in Figure 1-6. Compared to the classic Rankine cycle, this cycle works at a low

temperature (< 232°C). It is thermally economical as Rankine heat is recovered from low-temperature sources such as solar energy, biomass, geothermal, and industrial waste heat applications [25].

In 1824, the notion of employing other working fluids instead of water in heat engines was proposed. Organic fluids produced from petroleum were employed in internal combustion engines for the first time in 1853 [26]. In 1895, Frank W. Ufeldt developed an alcohol-water combination technique for ship propulsion. In the late 1950s, this cycle was developed by Lucien Brunecki and Hari Zvi Tabor in Naphtha engines, which are similar to ORC engines in principle for other applications, and were in use as early as the 1890s [27].

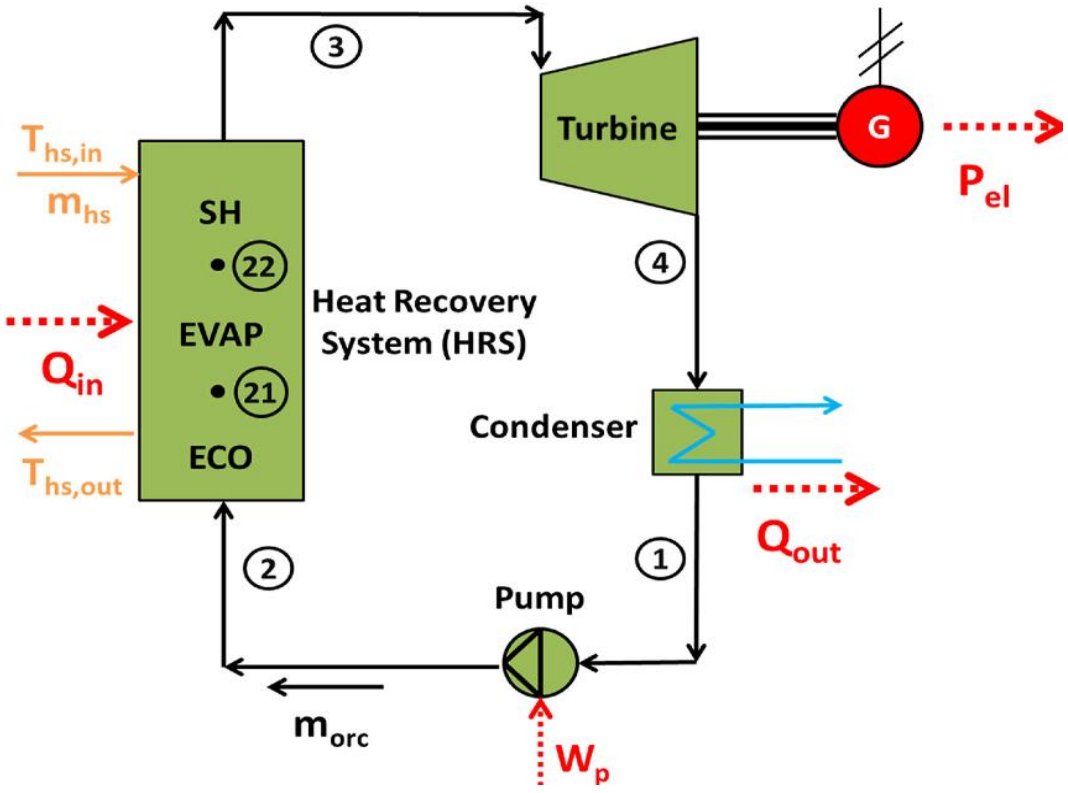

Figure 1.6. Schematic of the Organic Rankine cycle that recovers heat from waste emissions [12].

1.7. COMBINED POWER PLANT

A gas turbine is used in the combined cycle energy system to operate the electric generator, and the heat lost by the turbine exhaust is used to generate steam. The steam

resulting from the waste heat is employed in steam turbines to increase electricity production. The increase in electrical efficiency due to the combined cycle system is 50-60%. This is a significant improvement over the simple open-cycle application, with an efficiency of approximately 33% [28].

The combined cycle power system is the best for most large onshore power plants. The technology has also been used in offshore installations for more than ten years. These offshore installations are designed with an open cycle gas turbine to save capital costs, volume, and low weight per megawatt. A comparison of energy efficiency with fuel costs per megawatt was found for the combined cycle system .It is suitable for stable load applications and less so for marine applications with variable or decreasing loads [29]. In a new "Green spaces" improvement that includes a combined cycle system design, the size of the gas turbine can be improved, and it may be smaller than an equivalent open cycle configuration. In addition, a waste heat recovery unit (WHRU) can supersede gas turbine silencers, thus easing some of the space and weight limitations. The remaining heat can be used in place of flaming heaters; thus, the overall system efficiency will improve. Therefore, using energy technology for the combined cycle depends on the heat and energy required for an installation. Combined cycle technology is considered to be more cost-effective for large factories. Waste heat from WHRU is used in other heating applications when heat demand is high. For this reason, there will be less heat left to generate power [30].

An upgrade of gas turbine generators from a simple open-cycle system to a complex and expensive combined cycle was undertaken. This modification is not common in offshore facilities. It is considered a complex project due to the space needed to integrate the steam turbine, the additional overhead weight, and the additional personnel on the platform to manage steam system operations [29].

A combined-cycle power system consists of the following equipment: gas turbines (GTs), waste heat recovery units (WHRU-SG) to generate steam, steam turbines (STs), and condensers in addition to auxiliary equipment. These are illustrated in Figure 1.8. A combined cycle power system uses a gas turbine, a WHRU-SG waste heat recovery unit, and a steam turbine generator [31].

Some technologies provide advantages such as highly efficient power generation, and this can be considered an alternative to the combined cycle system:

- Organic Rankine cycle (ORC)
- Aeronautical gas turbines
- Offshore electricity (acquiring power from the shore)

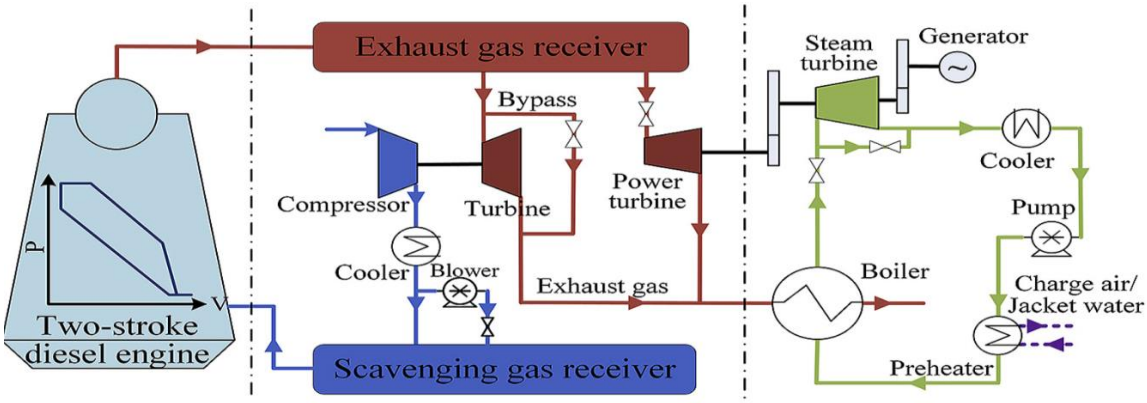

Figure 1.7. Combined cycle consisting of a gas turbine generator with a waste heat recovery unit and a steam turbine generator [32].

1.8. OBJECTIVES

- Power plant modeling for a combined cycle facility that would be added to an existing Taji power station site.
- Evaluate the design and operational parameters that affect the performance combined cycle (GSO CC).
- Examine energy performance, exergy efficiency, and power generation using thermodynamic and thermo-economic analysis.

1.9. THESIS STRUCTURE

This study is divided into five primary sections. Information about GSO CC and waste heat recovery and its uses are presented in the first section. Examples of GSO CC and waste heat recovery from thermodynamic cycles in earlier literature are presented in the second section. The GSO CC model used in this study and its design are discussed

in the third section. The fourth section examines the key findings of the GSO CC model and identifies the best outcomes for the selected model. The primary topic of this research and upcoming work is introduced in the fifth section.

PART 2

LITERATURE REVIEW

There are various studies in the literature on the organic Rankine cycle (ORC) [33–36] and the natural gas combined cycle (NGCC) [37–39]. Numerous articles have been published on the performance of the organic Rankine cycle generating power from a low-grade heat source, the energy analysis of the cycle, the exergy analysis, system optimization, the effects on the system performance depending on the properties of different working fluids, and the selection of the appropriate working fluid. There are publications on the energy and exergy analysis of the NGCC and the determination of optimum operating conditions. However, there are few studies on the performance of the combined two cycles [30,40].

Cihan [41] reported a thermodynamic analysis of a system that integrated the ORC utilizing waste heat and the conventional vapor compression refrigeration cycle. In the study, R600, R600a and R601 were chosen as refrigerants and power cycle efficiency and COP values were calculated. However, a performance comparison was made with R245fa fluid. As a result, it was determined that the most suitable fluid for the modeled system was R601.

Wei et al. [42] analyzed and optimized the performance of the ORC utilizing R245fa as the working fluid. They studied the thermodynamic performance of the ORC system under various situations. In their study, it was concluded that using as much waste heat as possible is the most effective method to increase the net power produced by the system.

Kaşka [43] performed energy and exergy analyses of the ORC. The researcher estimated the energy and exergy efficiencies for two distinct operating circumstances using actual data. In the first instance, the energy efficiency of the system, which drew

2,479 kW of energy from the furnace cooling water, was 10.2%, whereas the exergy efficiency was 48.5%. The energy efficiency of the second system, which pulled 2,208 kW of energy from the furnace cooling water, was 8.8%, whereas the exergy efficiency was 42.2%. In addition, he determined that the evaporator pressure significantly affects both energy and exergy efficiency. Pinch point analysis was also included in the study.

Mago et al. [44] looked at the ORC, which uses waste heat to create electricity, using Second Law analysis. Different fluids were used in the ORC to explore the influence of the boiling temperature of the fluid. The researchers worked on R113, R134a, R245ca, R123, R245fa, propane, and isobutane with boiling temperatures between -43°C and 48°C. The results were compared under the same conditions by selecting the working fluid water. First and Second Law analyses were applied by changing the operating parameters of the system at different reference temperatures. This investigation discovered that R113 has the most efficiency in organic fluids chosen above 430 K, while R245ca, R123, and R245fa have the highest efficiency in fluids selected between 380 and 430 K. In the study, it was also revealed that isobutane had the best efficiency below 380 K. As a result, it was stated that the boiling temperature of an organic fluid significantly affects the thermal efficiency of the system.

Liu et al. [45] conducted an ORC performance study based on the parameters of the working fluids. The researchers evaluated the impact of various working fluids on heat recovery and thermal efficiency. It was deduced that the critical temperature affects the thermal efficiency of various working fluids. It was found that the optimal evaporation temperature, which is somewhere between the waste heat inflow temperature and the condensation temperature, yields the highest heat recovery efficiency value. They also demonstrated that a higher entrance temperature for the waste heat source resulted in a higher maximum value of heat recovery efficiency.

Roy et al. [46] analyzed the performance of the ORC heat recovery system and optimized its parameters. R123, R12 and R134a were used as working fluids. A 312 kg/s flow rate and a 140°C flue gas temperature were used as a heat source. The findings revealed that the highest power and highest efficiency are obtained in the

cycle using R123 fluid. They calculated that when the pinch point temperature is 5°C and the flow rate is 341.16 kg/s, the power that can be produced is 19.09 MW, with First Law efficiency being 25.3% and Second Law efficiency 64.4%.

Zhang et al. [47] used vehicle exhaust gas as a waste heat source. They investigated the performance of several working fluids using a thermodynamic model derived from Matlab and REFPROP software. The selection of nine distinct organic fluids was based on their physical and chemical properties. The net power generation was kept constant at 10 kW and the results were compared with each other. The study assessed the environmental effect and safety level of the fluids. The results showed that the R141b, R11, R123, and R113 fluids perform slightly better in terms of thermodynamics than the other fluids. However, they discovered that R245ca and R245fa fluids are better for the environment in the application of engine waste heat recovery.

Wang et al. [48] evaluated the performance of the ORC generating power from waste heat with working fluids of R123, ammonia, water, butane, isobutane, R123, R11, R141B. R236EA, R113, and R245CA. They investigated the influence of thermodynamic factors on the ORC system's performance. The exergy efficiency of the ORC's thermodynamic parameters was calculated for each working fluid's optimization. Under the same conditions, the optimal performances of several fluids were compared and assessed. Their study concluded that the cycle powered by the organic fluid is better than the cycle powered by water. They found that the R236EA fluid has the highest exergy efficiency in the cycle.

Sun et al. [49] performed a performance analysis of ORC using different organic fluids between the crucial temperatures of organic fluids and the performance parameters of ORC (condensation pressure, evaporation pressure, hot fluid outlet temperature, net power, exergy efficiency, thermal efficiency, irreversibility loss of the cycle, heat recovery efficiency). It depended on the characteristics of the hot fluid passing through the evaporator under certain operating conditions. Based on this, relationships were constructed and confirmed at various evaporation and inflow temperatures of the hot

fluid. The researchers demonstrated that the performance characteristics of the organic fluid alter with its critical temperature.

Tyagi and Chen [50] evaluated the performance of the Brayton cycle with an irreversible regenerator based on the thermo-economic function. They defined the thermo-economic function as the sum of the total cost of the power produced and the system's operating cost divided by the maintenance cost. They optimized the thermo-economic function according to the cycle temperature. They determined the best performance characteristics under normal working situations. It was discovered that the influence of compressor efficiency was greater than the effect of the turbine efficiency on all performance measures.

Chen et al. [51] presented the optimum criterion for an intercooled Brayton cycle with an irreversible regenerator based on an ecological function. They defined the ecological function as the difference between the power produced and the loss of energy due to irreversibility. They estimated the best performance parameters for normal operating situations by maximizing the ecological function based on the cycle temperature. They discovered the optimal values for the turbine outlet temperature as well as the intercooling and cycle pressure ratios when the cycle performs optimally. However, they demonstrated that the optimal values of these parameters vary according on the cycle parameters, such as intercooler, turbine output temperature, cycle pressure ratios, and so on. As a consequence, they established optimal settings for intercooling, turbine output temperature, and cycle pressure ratios.

Al-Doori [52] studied the gas turbine power plant model with an intercooler. The impacts of the operating condition and design parameters on specific fuel consumption, thermal efficiency, and generated power were evaluated. The researcher stated that the efficiency increased when the power plant with an intercooler was compared with the power plant without an intercooler.

Tyagi et al. [22] optimized the power and efficiency of the Brayton cycle based on the cycle temperature. They calculated the optimum performance parameters under typical

operating conditions and found the optimal values of reheating, intercooling, and loop pressure ratios when the cycle reaches maximum performance.

Al-Sood et al. [53] demonstrated the performance of the gas turbine cycle with an irreversible regenerator, intercooling and reheating in different design and operating parameters. They attempted to find the optimum points that would provide the best performance for the gas turbine cycle. A mathematical simulation model was created to determine the performance characteristics of the cycle under various operating conditions. The model they developed provided the gas turbine cycle's best operating conditions (maximum First and Second Law efficiency, maximum ecological coefficient of performance, maximum generated power and minimum exergy loss).

Tyagi et al. [54] calculated the optimal operating settings of the Brayton cycle with an irreversible regenerator and intercooler to achieve the highest ecological coefficient of performance and produced power. They defined the ecological performance coefficient as the power produced divided by the usability loss. In the current operating conditions, the thermal efficiency and ecological coefficient of performance were optimized according to cycle pressure ratios, and intercooling. Maximum generated power, maximum efficiency, maximum ecological performance coefficient, and corresponding temperatures were calculated for given intercooling pressure ratios and other parameters under different operating conditions. The results indicated the optimum turbine outlet temperature, cycle pressure ratios, and intercooling when these performance parameters (such as generated power, thermal efficiency, and ecological coefficient of performance) reached their maximum values.

Zhang et al. [55] investigated the exergy analysis of Brayton and reversed the Brayton cycle with a combined regenerator. They derived exergy losses and exergy efficiencies. Based on the maximum exergy efficiency, they aimed to optimize the reverse Brayton cycle pressure ratio and obtain the corresponding optimum exergy efficiency. They analyzed the effects of various parameters on exergy efficiency with numerical calculations.

Abadi et al. [56] used different organic fluids in the system consisting of a combination of a gas turbine and ORC. First and Second Law analyses were performed for the selected organic fluids. From the results, it was determined that the efficiency of R245fa, propane and R152a fluids was higher at low temperatures. However, they determined that the efficiency of R113 fluid is maximum for temperatures above 100^{o}C.

Wang et al. [57] studied a double ORC for discontinuous heat recovery. Optimum operating conditions were calculated for butane, acetone, isopentane, pentane, R21, R141b, and R245fa fluids. A pinch point analysis was also performed to analyze the performance of the ORC. According to the findings of the research, dry and isentropic fluids performed the best.

Hung et al. [58] attempted to identify the best working fluids for the ORC employed in low-grade waste heat recovery. In their studies, it was determined that isentropic fluids are the best choice for heat recovery from low temperature sources.

Song et al. [59] analyzed the ORC and the integrated supercritical CO_2 Rankine cycle for WHR. In this study, the researchers revealed that the ORC subsystem significantly recovered the waste heat from the upper system operating under supercritical conditions.

Chacartegui et al. [60] suggested the use of ORC as a subsystem in combined power systems. The effects of using ORC as a subcycle in the combined system were investigated. The organic fluids R245, R113, isobutane, cyclohexane, toluene, isopentane, and cyclohexane were used. In the study, it was revealed that the efficiency of the combined organic Rankine cycle system working with Toluene and Cyclohexane fluid is high.

Lu et al. [61] examined combined power cycles in geothermal systems from a thermodynamic and techno-economic standpoint. A thermodynamic analysis of four power generating systems, namely the single flash system, the double flash system, the flash-ORC system, and the dual flash-ORC system, was performed in this work.

Optimization was performed using system comparisons to boost the net power production of the systems by 20%. R123, isobutane, R152a, R245fa, and n-pentane working fluids were used in each system with the aim to select optimum geothermal energy cycles under different geothermal fluid conditions. In the techno-economic analysis, electricity level costs and payback periods were evaluated. The power level costs and payback durations were examined in the techno-economic study.

Yang et al. [62] created heat transfer, thermodynamic, and optimization models for the ORC-ORC combined power system to regain the exhaust waste heat from the cooling system and intercooler waste heat of a six-cylinder CNG (compressed natural gas) engine. Thermodynamic and heat transfer performances were solved using the Pareto method and a GA (genetic algorithm) in order to maximize the net power output and minimize the heat transfer area in accordance with the waste heat characteristics of the CNG engine over the entire operating range. With this analysis, they determined the optimum operating range of the system. In the analysis, they also concluded that the optimum evaporation pressure of the high temperature cycle and the degree of overheating were affected by the operating conditions of the CNG engine.

Zhang et al. [63] carried out a comparative thermodynamic analysis of three power systems by utilizing the relatively low-to-moderate waste heat in the temperature range of 150 to 350°C of the combined cycle of the steam Rankine cycle, the ORC and the steam-ORC integrated. According to the analysis results, the heat source was at a temperature of 150-210°C. Maximum thermal efficiency, exergy efficiency and power generation were calculated for the ORC system. In the heat source conditions with a temperature range of 21 to 350°C, the integrated system had far higher thermal efficiency, exergy efficiency and power generation values than other systems.

Ataei et al. [64] analyzed different cycle applications using R113, RC318, iso-pentane and n-hexane dry organic fluids. ORC configurations: a basic ORC is an ORC with regenerative ORC, an internal heat exchanger, and a regenerative ORC with an internal heat exchanger. This was simulated using EES for various ambient temperatures. In addition, an environmental performance assessment was made. In conclusion, the regenerative ORC with an internal heat exchanger had the best performance values

with a thermal efficiency of 21.7% and a Second Law efficiency of 64.2%. N-hexane was proven to be the most efficient working fluid for the cycle. In addition, both thermal efficiency and Second Law efficiency rose as the temperature outside dropped.

Mohapatra and Sanjay [65] examined the effects of cooling the gas turbine inlet with various techniques for combined cycle configurations (CCCs) and outlined the advantages and disadvantages of these techniques. The results of these techniques were examined for both gas and CCCs and interpreted according to various ambient conditions. In the results of working, it was observed that the system, which performs cooling by steam pressurization, provides an improvement of 9.47% in gas cycle efficiency and 17.2% in power output, and is recommended for CCCs systems. As a result of the studies, the optimum inlet temperature was found to be 20°C.

PART 3

METHODOLOGY

3.1. MODEL DESCRIPTION

In this thesis, a model is prepared and discussed for the steady-state analysis of the natural gas combined cycle which is integrated with the organic Rankine cycle (GSO CC). It includes three main parts. The first part is the Brayton cycle, which consists of a gas turbine (GT), a combustion chamber (CC), and an air compressor (AC). The second part, which represents the Rankine cycle, consists of two pumps (P1 and P2), a deaerator, a condenser (CON1), a steam turbine (ST), and heat recovery steam generation (HRSG). The third and final part of the Organic Rankine cycle consists of a heat exchanger (HE), an organic Rankine turbine (ORT), a condenser (CON2), a pump (P3), and a heat recovery boiler (HRB) (see Figure 3.1). The principle of operation of the embedded system can be summarized as follows.

Air is compressed to operating pressure and heated as it enters an air compressor (AC). The air is then transported to the CC, reacting with the natural gas fuel to create high-pressure, high-temperature exhaust gases. Through the GT, the exhaust gases expand to produce mechanical power. The HRSG converts compressed water into steam at high temperatures using the temperature of the exhaust gases. To generate more mechanical power, the steam expands as it passes through the ST. The water is pressurized through the pump after entering the condenser, which turns all the vapor into saturated liquid.

The working principle of the organic Rankine cycle is similar to that of the Rankine cycle: the working fluid is pumped into a heat recovery boiler where it evaporates, passes through an expansion device (the turbine), then through a condenser heat exchanger where it is finally re-condensed.

The selection of the working fluid is essential. R123 was chosen as the working fluid in this current work because it is the most suitable fluid dynamically and economically. It is environmentally friendly with an acceptable value of ODP and low global warming value compared to other working fluids. Additionally, R123 falls into the category of dry working fluids with a higher critical temperature value (in relatively lower certainty ranges) which makes it a suitable working fluid in ORC applications. Moreover, R123 is the most suitable working fluid in ORCs for engine or gas turbine WHRT applications and is highly recommended by many researchers, given all of the above R123 environmental and technical advantages.

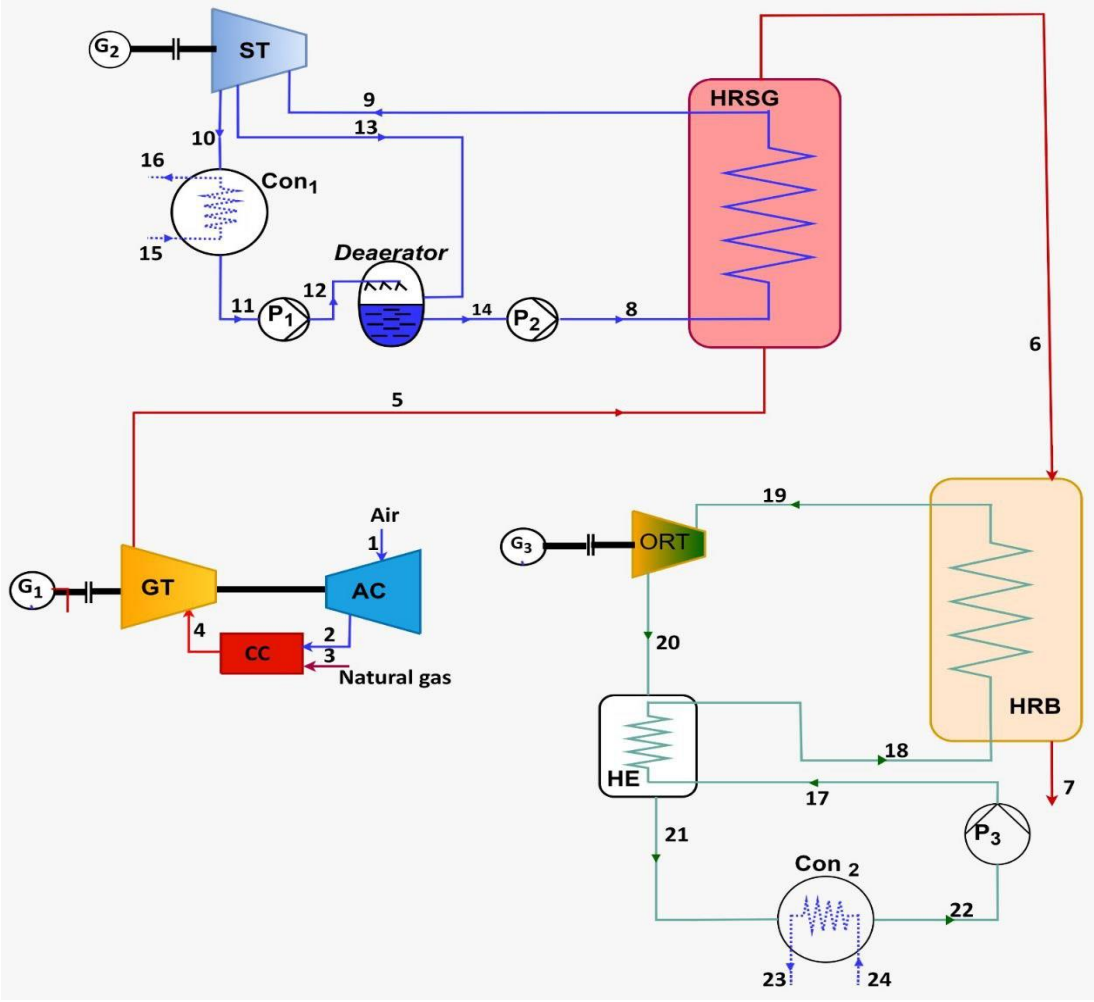

Figure 3.1. Schematic diagram of the GSO CC.

3.2 GENERAL EQUATIONS OF MASS, ENERGY AND EXERGY

The conservation of mass equation for an SSSF open system is [18]:

$$\sum \dot{m}_{in} = \sum \dot{m}_{out} \quad 3\text{-}1$$

where:

$\sum \dot{m}_{in}$ is the total mass flow entering per unit of time, and
$\sum \dot{m}_{out}$ is the total mass flow exiting per unit time.

The energy balance for each component is based on the First Law of Thermodynamics for an SSSF open system [19,66]:

$$\dot{Q} + \dot{W} = \sum \dot{m}_{out} h_{out} - \sum \dot{m}_{in} h_{\text{in}} \quad 3\text{-}2$$

where:

$\dot{Q}$ is the heat transfer per unit time,
$\dot{W}$ is the work done by the control volume per unit time,
h_{in} is the specific enthalpy per the mass entering the system, and
h_{out} is the specific enthalpy per mass leaving the system.

Unlike mass and energy, entropy is not conserved in open and closed systems, as entropy is produced due to irreversibility. In open systems, the entropy balance can be expressed as [17]:

$$\dot{E} = \dot{m}\psi \quad 3\text{-}3$$

$$\psi = (h - h_0) - T_0(s - s_0) \quad 3\text{-}4$$

where:

s_0 is the specific entropy of the mass entering the open system,
s is the specific entropy of the mass emanating from the open system,

T_0 is the boundary temperature between the open system and the environment,

$\dot{E}$ is the exergy flows, and

ψ is the specific exergy.

Energy analysis does not provide information about system irreversibility due to entropy generation and exergy destruction. Therefore, considering the Second Law of Efficiency, the thermodynamic performance of GSO CC cycle systems should be done. Exergy will be helpful to take advantage of the system when a final firsthand regimen with the environment is acquired.

3.3. THERMODYNAMIC ANALYSIS OF THE BC MODEL

3.3.1. Compressor Model

Air compressor machines that use power to create kinetic energy compress and pressurize air and may release it in short bursts [67,68]. Rotary compressors are required due to the significant flow rates of turbines and their comparatively low-pressure ratios. The energetic relation for the compressor model is modified as follows [69,70]:

(a) Energy balance:

$$\dot{W}_{AC} = \dot{m}_{\text{air}} (h_2 - h_1) \quad \text{3-5}$$

$$\eta_{AC} = \frac{\dot{W}_{AC,s}}{\dot{W}_{AC}} \quad \text{3-6}$$

(b) Isentropic efficiency:

The exergetic relations for the compressor model are modified as follows:

(c) Exergy balance:

$$\dot{E}_{D,AC} = \left(\dot{E}_1 - \dot{E}_2\right) + \dot{W}_{AC} \quad (3\text{-}7)$$

Exergy efficiency:

$$\dot{E}_{f,AC} = \dot{E}_2 - \dot{E}_1 \quad (3\text{-}8)$$

$$\dot{E}_{P,AC} = \dot{W}_{\mathrm{AC}} \quad (3\text{-}9)$$

$$\varepsilon_{\mathrm{AC}} = \frac{\dot{E}_{P,AC}}{\dot{E}_{f,AC}} = 1 - \frac{\dot{E}_{\mathrm{D,AC}}}{\dot{E}_{f,AC}} \quad (3\text{-}10)$$

where:

$\dot{E}_{P,AC}$ is the product exergy for the compressor,
$\dot{E}_{f,AC}$ is the fuel exergy for the compressor, and
$\varepsilon_{\mathrm{AC}}$ is the exergy efficiency exergy for the compressor.

3.3.2. Combustion Chamber Model

The combustion chamber is the area of the gas turbine where energy is introduced. The combustor is the source of energy for the gas turbine cycle. It takes in air, adds fuel, combines the two, and then allows the mixture to burn. This procedure is often carried out under continuous pressure (although small pressure losses are generally present) [71]. Temperature is a crucial characteristic during combustion and material qualities usually restrict it. The materials must be resistant to extreme temperatures and temperature gradients. Otherwise, the gas turbine may fail [72].

The energetic relation for the combustion chamber model is modified as follows:

(a) Energy balance:

$$\dot{m}_2 h_2 + \eta_{CC} \dot{m}_3 \text{LHV} = \dot{m}_4 h_4 \quad \text{3-11}$$

The exergetic relations for the combustion chamber model are modified as follows:

(b) Exergy balance:

$$\dot{E}_{\text{D,CC}} = \dot{E}_2 + \dot{E}_3 - \dot{E}_4 \quad \text{3-12}$$

(c) Exergy efficiency:

$$\dot{E}_{p,CC} = \dot{E}_4 \quad \text{3-13}$$

$$\dot{E}_{f,CC} = \dot{E}_2 + \dot{E}_3 \quad \text{3-14}$$

$$\varepsilon_{\text{CC}} = \frac{P_{\text{CC}}}{F_{\text{CC}}} = 1 - \frac{\dot{E}_{\text{D,CC}}}{\dot{E}_{f,CC}} \quad \text{3-15}$$

3.3.3. Gas turbine Model

All gas turbines are designed as a convergent duct, where gaseous energy is not supplied nor removed but transformed from pressure and temperature into velocity. As air moves from a large intake into a smaller exit, the velocity of the air increases [73][15]. At higher speeds, impact pressure rises. The overall pressure in the system stays constant, and static pressure drops since energy is neither supplied nor withdrawn [74]. This may be viewed as static pressure being converted to impact pressure such that an increase in static pressure is accompanied by a flow of air via a convergent duct and expansion. Any expansion results in a corresponding temperature decrease.

The energetic relation for the gas turbine model is modified as follows:

(a) Energy balance:

$$\dot{W}_{GT} = \dot{m}_{gas}(h_4 - h_5) \quad \text{3-16}$$

(b) Isentropic efficiency:

$$\eta_{GT} = \frac{\dot{W}_{GT}}{\dot{W}_{GT,s}} \quad \text{3-17}$$

The exergetic relations for the gas turbine model are modified as follows:

(c) Exergy balance:

$$\dot{E}_{D,GT} = \left(\dot{E}_4 - \dot{E}_5\right) - \dot{W}_{GT} \quad \text{3-18}$$

(d) Exergy efficiency:

$$\dot{E}_{P,GT} = \dot{W}_{GT} \quad \text{3-19}$$

$$\dot{E}_{F,GT} = \dot{E}_4 - \dot{E}_5 \quad \text{3-20}$$

$$\varepsilon_{\mathrm{GT}} = \frac{P_{\mathrm{GT}}}{F_{\mathrm{GT}}} = 1 - \frac{\dot{E}_{\mathrm{D,GT}}}{\dot{E}_{F,GT}} \quad \text{3-21}$$

3.4. THERMODYNAMIC ANALYSIS OF THE RC MODEL

3.4.1. HRSG Model

An HRSG is a set of heat exchangers that operate in a series. Heat exchangers, known in some circles as steam turbines, use heat to produce steam. Both natural and forced circulation systems may be installed on an HRSG [75]. Hot exhaust runs over the tubes, which heats the water within them, resulting in steam production. Creating dry

superheated steam is an involved process, with each of the modules intended for a specific function. All modules are known as economizers, evaporators, super heaters/reheaters, and preheaters [76].

The temperature of the steam produced in the waste heat recovery boilers is closely related to the temperature of the exhaust gas. If the exhaust gas temperature is insufficient to produce the desired steam temperature, additions such as auxiliary burners are made to the boiler [77]. The energetic relation for the HRSG model is modified as follows:

(a) Energy balance:

$$\dot{m}_5 + \dot{m}_8 = \dot{m}_6 + \dot{m}_9 \quad (3\text{-}22)$$

$$\dot{Q}_{HRSG} = \dot{m}_8(h_9 - h_8) \quad (3\text{-}23)$$

The exergetic relations for the HRSG model are modified as follows:

(b) Exergy balance:

$$\dot{E}_{\mathrm{D,HRSG}} = \dot{E}_5 - \dot{E}_6 + \dot{E}_8 \quad (3\text{-}24)$$

(c) Exergy efficiency:

$$\dot{E}_{P,HRSG} = \dot{E}_9 - \dot{E}_8 \quad (3\text{-}25)$$

$$\dot{E}_{F,HRSG} = \dot{E}_5 - \dot{E}_6 \quad (3\text{-}26)$$

$$\varepsilon_{\mathrm{HRSG}} = \frac{P_{\mathrm{HRSG}}}{F_{\mathrm{HRSG}}} = 1 - \frac{\dot{E}_{\mathrm{D,HRSG}}}{\dot{E}_{F,HRSG}} \quad (3\text{-}27)$$

3.4.2. Steam Turbine Model

The steam turbine's purpose is to transform the steam's thermal energy into mechanical energy. The steam is delivered from the first expansion area of the turbine to the blades on the rotor and expands to the condensing pressure. The rotten steam passes from the turbine body to the condenser [78]. The energetic relation for the steam turbine model is modified as follows:

Energy balance:

$$\dot{W}_{\mathrm{ST}} = \dot{m}_9(h_9 - h_{13}) + \dot{m}_{10}(h_{13} - h_{10}) \quad \text{3-28}$$

(a) Isentropic efficiency:

$$\eta_{ST} = \frac{\dot{W}_{ST}}{\dot{W}_{ST\,,s}} \quad \text{3-29}$$

The exergetic relations for the steam turbine model are modified as follows:

(a) Exergy balance:

$$\dot{E}_{\mathrm{D,ST}} = \left(\dot{E}_9 - \dot{E}_{13} - \dot{E}_{10}\right) - \dot{W}_{\mathrm{ST}} \quad \text{3-30}$$

(b) Exergy efficiency:

$$\dot{E}_{P,ST} = \dot{W}_{ST} \quad \text{3-31}$$

$$\dot{E}_{F,ST} = \dot{E}_9 - \dot{E}_{10} - \dot{E}_{13} \quad \text{3-32}$$

$$\varepsilon_{\mathrm{ST}} = \frac{P_{\mathrm{ST}}}{F_{\mathrm{ST}}} = 1 - \frac{\dot{E}_{\mathrm{D,ST}}}{\dot{E}_{F,ST}} \quad \text{3-33}$$

3.4.3. Condenser Model

Condensers are heat exchangers and their purpose is to convert used steam from the turbine body into water by condensing it with the help of cooling water. Water-cooled condensers are preferred in vapor power plants because of the condensing pressure being lower than an air-cooled system. Moreover, it is easier to control the condensing pressure and there is higher heat transfer due to the high heat capacity of water [79]. The energetic relation for the condenser model is modified as follows:

(a) Energy balance:

$$\dot{m}_{10} + \dot{m}_{15} = \dot{m}_{11} + \dot{m}_{16} \quad \text{3-34}$$

$$\dot{Q}_{COND1} = \dot{m}_{10}(h_{11} - h_{10}) \quad \text{3-35}$$

The exergetic relations for the condenser model are modified as follows:

(a) Exergy balance:

$$\dot{E}_{\mathrm{D},\,COND1} = \left(\dot{E}_{10} - \dot{E}_{11}\right) + \left(\dot{E}_{15} - \dot{E}_{16}\right) \quad \text{3-36}$$

(b) Exergy efficiency:

$$\dot{E}_{P,COND1} = \dot{E}_{16} - \dot{E}_{15} \quad \text{3-37}$$

$$\dot{E}_{F,COND1} = \dot{E}_{10} - \dot{E}_{11} \quad \text{3-38}$$

$$\varepsilon_{COND1} = \frac{P_{COND1}}{F_{COND1}} = 1 - \frac{\dot{E}_{\mathrm{D},COND1}}{\dot{E}_{F,COND1}} \quad \text{3-39}$$

3.4.4. Pump Model

The feed-water pump must absorb the pressurized water needed for steam production from the feed tank and send it to the system. Compressors and pumps are comparable in that they both boost pressure in a fluid and push it through a pipe. Compressible gases are reduced in volume when the compressor compresses them. Liquids are difficult to compress. While some are easier to pressurize, pumps mostly work to pressurize and move liquids [80]. The energetic relations for the pump model are modified as follows:

(a) Energy balance:

$$\dot{W}_{\text{Pump1}} = \dot{m}_{11}(h_{12} - h_{11}) \quad \text{3-40}$$

$$\dot{W}_{\text{Pump2}} = \dot{m}_{8}(h_{14} - h_{8}) \quad \text{3-41}$$

(b) Isentropic efficiency:

$$\eta_{\text{Pump1}} = \frac{\dot{W}_{\text{Pump1},s}}{\dot{W}_{\text{Pump1}}} \quad \text{3-42}$$

$$\eta_{\text{Pump2}} = \frac{\dot{W}_{\text{Pump2},s}}{\dot{W}_{\text{Pump2}}} \quad \text{3-43}$$

The exergetic relations for the pump are modified as follows:

(c) Exergy balance:

$$\dot{E}_{\text{D, Pump1}} = \dot{W}_{\text{Pump1}} - \left(\dot{E}_{11} - \dot{E}_{12}\right) \quad \text{3-44}$$

$$\dot{E}_{\text{D, Pump2}} = \dot{W}_{\text{Pump2}} - \left(\dot{E}_{14} - \dot{E}_{8}\right) \quad \text{3-45}$$

$$\dot{E}_{P,PUMP1} = \dot{E}_{12} - \dot{E}_{11} \quad (3\text{-}46)$$

$$\dot{E}_{F,PUMP1} = \dot{W}_{\text{Pump1}} \quad (3\text{-}47)$$

$$\varepsilon_{\text{Pump1}} = \frac{P_{\text{Pump1}}}{F_{\text{Pump1}}} = 1 - \frac{\dot{E}_{\text{D, Pump1}}}{\dot{E}_{F,PUMP1}} \quad (3\text{-}48)$$

$$\dot{E}_{P,PUMP2} = \dot{E}_{8} - \dot{E}_{14} \quad (3\text{-}49)$$

$$\dot{E}_{F,PUMP2} = \dot{W}_{\text{Pump2}} \quad (3\text{-}50)$$

$$\varepsilon_{\text{Pump2}} = \frac{P_{\text{Pump2}}}{F_{\text{Pump2}}} = 1 - \frac{\dot{E}_{\text{D, Pump2}}}{\dot{E}_{F,PUMP2}} \quad (3\text{-}51)$$

3.4.5. Deaerator Model

Thermal deaerators are used to remove dissolved gases in the feed water of steam-generating boilers on a large scale. Dissolved oxygen in the feed water causes corrosion damage to the boiler and the formation of oxides (such as rust) by binding to the walls of metal pipes and other equipment. Low-pressure steam is obtained from an extraction point in the steam turbine system. Deaerators use this low-pressure steam in steam generation systems in most thermal power plants. However, steam generators can use low-pressure steam in many large industrial plants, such as petroleum refineries. The energetic relation for the condenser model is modified as follows:

(a) Energy balance:

$$\dot{m}_{13}h_{13} + \dot{m}_{12}h_{12} = \dot{m}_{14}h_{14} \quad (3\text{-}52)$$

The exergetic relations for the condenser model are modified as follows:

(a) Exergy balance:

$$\dot{E}_{\text{D, Deaerator}} = \dot{E}_{13} + \dot{E}_{12} - \dot{E}_{14} \quad (3\text{-}53)$$

(b) Exergy efficiency:

$$\dot{E}_{P,\text{ Deaerator}} = \dot{E}_{14} \quad (3\text{-}54)$$

$$\dot{E}_{F,\text{ Deaerator}} = \dot{E}_{13} + \dot{E}_{12} \quad (3\text{-}55)$$

$$\varepsilon_{\text{Deaerator}} = \frac{P_{\text{Deaerator}}}{F_{\text{Deaerator}}} = 1 - \frac{\dot{E}_{\text{D, Deaerator}}}{\dot{E}_{F,\text{ Deaerator}}} \quad (3\text{-}56)$$

3.5. THERMODYNAMIC ANALYSIS OF THE ORC MODEL

3.5.1. HRB Model

The energetic relation for the HRB model is modified as follows:

(a) Energy balance:

$$\dot{m}_6 + \dot{m}_{18} = \dot{m}_7 + \dot{m}_{19} \quad (3\text{-}57)$$

$$\dot{Q}_{HRB} = \dot{m}_{18}(h_{19} - h_{18}) \quad (3\text{-}58)$$

The exergetic relations for the HRB model are modified as follows:

(b) Exergy balance:

$$\dot{E}_{\text{D},HRB} = \dot{E}_6 - \dot{E}_7 + \dot{E}_{18} - \dot{E}_{19} \quad (3\text{-}59)$$

(c) Exergy efficiency:

$$\dot{E}_{P,HRB} = \dot{E}_{19} - \dot{E}_{18} \quad (3\text{-}60)$$

$$\dot{E}_{F,HRB} = \dot{E}_6 - \dot{E}_7 \quad (3\text{-}61)$$

$$\varepsilon_{HRB} = \frac{P_{HRB}}{F_{HRB}} = 1 - \frac{\dot{E}_{\mathrm{D},HRB}}{\dot{E}_{F,HRB}} \quad (3\text{-}62)$$

3.5.2. ORT Model

The energetic relation for the ORT turbine model is modified as follows:

(a) Energy balance:

$$\dot{W}_{\mathrm{ORT}} = \dot{m}_{19}(h_{20} - h_{19}) \quad (3\text{-}63)$$

(b) Isentropic efficiency:

$$\eta_{\mathrm{ORT}} = \frac{\dot{W}_{\mathrm{ORT},s}}{\dot{W}_{\mathrm{ORT}}} \quad (3\text{-}64)$$

The exergetic relations for the ORT model are modified as follows:

(c) Exergy balance:

$$\dot{E}_{\mathrm{D,ORT}} = \left(\dot{E}_{19} - \dot{E}_{20}\right) - \dot{W}_{\mathrm{ORT}} \quad (3\text{-}65)$$

(d) Exergy efficiency:

$$\dot{E}_{P,ORT} = \dot{E}_{19} - \dot{E}_{20} \quad (3\text{-}66)$$

$$\dot{E}_{F,ORT} = \dot{W}_{\mathrm{ORT}} \quad (3\text{-}67)$$

$$\varepsilon_{\mathrm{ORT}} = \frac{P_{\mathrm{ORT}}}{F_{\mathrm{ORT}}} = 1 - \frac{\dot{E}_{\mathrm{D,ORT}}}{\dot{E}_{F,ORT}} \quad (3\text{-}68)$$

3.5.3. ORC Condenser Model

The energetic relation for the condenser model is modified as follows:

(a) Energy balance:

$$\dot{m}_{21} + \dot{m}_{24} = \dot{m}_{22} + \dot{m}_{23} \quad \text{3-69}$$

$$\dot{Q}_{COND2} = \dot{m}_{21}(h_{22} - h_{21}) \quad \text{3-70}$$

The exergetic relations for the condenser model are modified as follows:

(a) Exergy balance:

$$\dot{E}_{\mathrm{D},\,COND2} = \left(\dot{E}_{21} - \dot{E}_{22}\right) + \left(\dot{E}_{23} - \dot{E}_{24}\right) \quad \text{3-71}$$

(b) Exergy efficiency:

$$\dot{E}_{P,COND2} = \dot{E}_{24} - \dot{E}_{23} \quad \text{3-72}$$

$$\dot{E}_{F,COND2} = \dot{E}_{21} - \dot{E}_{22} \quad \text{3-73}$$

$$\varepsilon_{COND2} = \frac{P_{COND2}}{F_{COND2}} = 1 - \frac{\dot{E}_{\mathrm{D},COND2}}{\dot{E}_{F,COND2}} \quad \text{3-74}$$

3.5.4. ORC Pump Model

The energetic relations for the ORC pump model are modified as follows:

(a) Energy balance:

$$\dot{W}_{\mathrm{Pump3}} = \dot{m}_{22}(h_{17} - h_{22}) \quad \text{3-75}$$

(b) Isentropic efficiency:

$$\eta_{\text{Pump3}} = \frac{\dot{W}_{\text{Pump3},s}}{\dot{W}_{\text{Pump3}}} \quad \text{3-76}$$

The exergetic relations for the ORC pump are modified as follows:

(c) Exergy balance:

$$\dot{E}_{\text{D, Pump3}} = \dot{W}_{\text{Pump3}} - \left(\dot{E}_{22} - \dot{E}_{17}\right) \quad \text{3-77}$$

(d) Exergy efficiency:

$$\dot{E}_{\text{P, Pump3}} = \dot{E}_{17} - \dot{E}_{22} \quad \text{3-78}$$

$$\dot{E}_{\text{F, Pump3}} = \dot{W}_{\text{Pump3}} \quad \text{3-79}$$

$$\varepsilon_{\text{Pump3}} = \frac{P_{\text{Pump3}}}{F_{\text{Pump3}}} = 1 - \frac{\dot{E}_{\text{D, Pump3}}}{\dot{E}_{\text{F, Pump3}}} \quad \text{3-80}$$

3.5.5. HEAT EXCHANGER Model

The energetic relation for the heat exchanger model is modified as follows:

(a) Energy balance:

$$\dot{m}_{17} + \dot{m}_{20} = \dot{m}_{18} + \dot{m}_{21} \quad \text{3-81}$$

$$\dot{Q}_{HE} = \dot{m}_{17}(h_{18} - h_{17}) \quad \text{3-82}$$

The exergetic relations for the HE model are modified as follows:

(b) Exergy balance:

$$\dot{E}_{\mathrm{D,HE}} = \dot{E}_{17} - \dot{E}_{18} + \dot{E}_{20} - \dot{E}_{21} \quad \text{3-83}$$

(c) Exergy efficiency:

$$\dot{E}_{\mathrm{P,\,HE}} = \dot{E}_{21} - \dot{E}_{20} \quad \text{3-84}$$

$$\dot{E}_{\mathrm{F,\,HE}} = \dot{E}_{17} - \dot{E}_{18} \quad \text{3-85}$$

$$\varepsilon_{\mathrm{HE}} = \frac{P_{\mathrm{HE}}}{F_{\mathrm{HE}}} = 1 - \frac{\dot{E}_{\mathrm{D,HE}}}{\dot{E}_{\mathrm{F,\,HE}}} \quad \text{3-86}$$

3.6. ECONOMIC ANALYSIS

The main costs of a thermal system are capital investment, maintenance and operation, and fuel. A simplified economic model can be applied based on the capital recovery factor (CRF). The total capital investment (TCI) in a plant is given by the sum of all purchased equipment costs (PEC) multiplied by a constant factor. The total capital investment in the plant is given by [81,82]:

$$\dot{Z}_k = \frac{Z_k \times CRF \times \phi}{N \times 3600} \quad \text{3-87}$$

where:

PEC is the equipment purchase cost in US dollars,
φ is the maintenance factor (1.06), and
CRF is the Capital Recovery Factor, which can be calculated thus:

$$\mathrm{CRF} = \frac{i(1+i)^n}{(1+i)^n - 1} \quad \text{3-88}$$

where:

i is the interest rate (considered to be 10%), and
n is the system lifetime (considered to be 20 years).

The purchase equipment cost (PEC) for the GSO CC components is as follows [82][83]:

Brayton Cycle

(a) Air Compressor [83]

$$PEC_{comp} = \left(\frac{71.1 \times \dot{m}_{air} \times \left(\frac{p_2}{p_1}\right)}{0.9 - \eta_{comp}} \right) \quad \text{3-89}$$

(b) Combustion Chamber

$$PEC_{cc} = \left(\frac{25.6 \times \dot{m}_{air}}{0.995 - \left(\frac{p_4}{p_2}\right)} \right) \times [1 + exp(0.018 \times T_4 - 26.4)] \quad \text{3-90}$$

(c) Gas Turbine

$$PEC_{GT} = \left(\frac{26.6 \times \dot{m}_{gas}}{0.92 - \eta_{GT}} \right) \times ln\left(\frac{p_4}{p_5}\right) \times [1 + exp(0.036 \times T_4 - 54.4)] \quad \text{3-91}$$

Rankine Cycle

(a) Heat Recovery Steam Generator

$$PEC_{HRSG} = 6570 \left[\left(\frac{\dot{Q}_{boiler}}{\Delta T} \right)^{0.8} \right] + 21276 \dot{m}_{water} + 1184.4 \dot{m}_g \quad \text{3-92}$$

(b) Steam Turbine

$$PEC_{ST} = 6000(W_{ST}^{0.7}) \quad \text{3-93}$$

(c) Condenser

$$PEC_{Cond} = 1773\dot{m}_{steam}^{\circ} \quad \text{3-94}$$

(d) Pump

$$PEC_{p} = 3540W_{p}^{0.7} \quad \text{3-95}$$

Organic Rankine Cycle

(a) Pump

$$\text{PEC}_{P} = 3540(\dot{W}_{P})^{0.71} \quad \text{3-96}$$

(b) Evaporator

$$\text{PEC}_{\text{Eva}} = 309.143(A_{\text{eva}}) + 231.915 \quad \text{3-97}$$

(c) Turbine

$$\text{PEC}_{T} = 6000(\dot{W}_{T}^{0.7}) \quad \text{3-98}$$

(d) Condenser

$$\text{PEC}_{\text{Cond}} = 1773(\dot{m}_{\text{Steam}}) \quad \text{3-99}$$

(e) Heat exchanger

$$\mathrm{PEC_{HE}} = 1.3(190 + 310A_{\mathrm{HE}}) \quad \text{3-100}$$

3.7. COST PERFORMANCE

The cost balance and auxiliary equations for each part must be written as follows [39]:

$$\sum_{e} \dot{C}_{e,k} + \dot{C}_{w,k} = \dot{C}_{q,k} + \sum_{i} \dot{C}_{i,k} + \dot{Z}_k \quad \text{3-101}$$

$$\dot{C}_j = c_j \dot{E}_j \quad \text{3-102}$$

where:

C is the cost rate (\$/h), and $\dot{Z}_k$ represents the entire cost rate related to capital investment and operation and maintenance costs component *k*.

Table 3.1 presents the relevant parameters for the exergo-economic assessment of the system. Table 3.2 contains the cost balances and auxiliary equations for every system component.

Table 3.1. Exergo-economic evaluation parameters of GT–HRSG/ORC [70].

Average costs per exergy unit of fuel	$\boldsymbol{c_{F,k} = \dot{C}_{F,k}/\dot{E}_{F,k}}$
Average costs per exergy unit of product	$c_{P,k} = \dot{C}_{P,k}/\dot{E}_{P,k}$
Cost rate of exergy destruction	$\dot{C}_{D,k} = c_{F,k}\dot{E}_{D,k}$
Relative Cost Difference	$r_k = \left(c_{P,k} - c_{F,k}\right)/c_{F,k}$
Exergo-economic factor	$f_k = \dot{Z}_k/\left(\dot{Z}_k + c_{F,k}\dot{E}_{D,k} + \dot{E}_{L,k}\right)\Big)$

Table 3.2. Cost analysis.

Component	Exergetic cost rate balance equation	Auxiliary Equation	
Compressor	$\dot{C}_1 + \dot{C}_{AC} + \dot{Z}_{\mathrm{AC}} = \dot{C}_2$	$\frac{\dot{C}_1}{\dot{W}_{\mathrm{C,LP}}} = \frac{\dot{C}_2}{\dot{W}_{\mathrm{T}}}$	$c_1=0$
Combustion chamber	$\dot{C}_2 + \dot{C}_3 + \dot{Z}_{\mathrm{CC}} = \dot{C}_4$	$\frac{\dot{C}_2}{\mathrm{Ex}_2} = \frac{\dot{C}_4}{\mathrm{Ex}_4}$	$c_2=c_4$ $c_3=12$
Gas turbine	$\dot{C}_4 + \dot{Z}_{\mathrm{GT}} = \dot{C}_5 + \dot{C}_{AC}$	$\frac{\dot{C}_4}{\mathrm{Ex}_4} = \frac{\dot{C}_5}{\mathrm{Ex}_5}$	$c_4=c_5$
HRSG	$\dot{C}_5 + \dot{C}_8 + \dot{Z}_{\mathrm{HRSG}} = \dot{C}_6 + \dot{C}_9$	$\frac{\dot{C}_5}{\mathrm{Ex}_5} = \frac{\dot{C}_6}{\mathrm{Ex}_6}$	$c_5 = c_6$
Steam turbine	$\dot{C}_9 + \dot{Z}_{ST} = \dot{C}_{10} + \dot{C}_{13} + \dot{C}_{ST}$	$\frac{\dot{C}_9}{\mathrm{Ex}_9} = \frac{\dot{C}_{10}}{\mathrm{Ex}_{10}}$	$c_9=c_{10}$ $c_{10}= c_{13}$
Condenser 1	$\dot{C}_{10} + \dot{C}_{15} + \dot{Z}_{\mathrm{cond1}} = \dot{C}_{11} + \dot{C}_{16}$	$\frac{\dot{C}_{10}}{\mathrm{Ex}_{10}} = \frac{\dot{C}_{11}}{\mathrm{Ex}_{11}}$	$c_{10}=c_{11}$ $c_{15}= 0$
Pump 1	$\dot{C}_{11} + \dot{C}_{ST} + \dot{Z}_{\mathrm{Pump1}} = \dot{C}_{12}$	$\frac{\dot{C}_{Pump1}}{\dot{W}_{\mathrm{Pump1}}} = \frac{\dot{C}_{ST}}{\dot{W}_{\mathrm{ST}}}$	
Dereatear	$\dot{C}_{12} + \dot{C}_{13} + \dot{Z}_{\mathrm{Derea}} = \dot{C}_{14}$	$\frac{\dot{C}_{12}}{\mathrm{Ex}_{12}} = \frac{\dot{C}_{14}}{\mathrm{Ex}_{14}}$	
Pump 2	$\dot{C}_{14} + \dot{C}_{ST} + \dot{Z}_{\mathrm{Pump2}} = \dot{C}_8$	$\frac{\dot{C}_{Pump2}}{\dot{W}_{\mathrm{Pump2}}} = \frac{\dot{C}_{ST}}{\dot{W}_{\mathrm{ST}}}$	
Evaporator	$\dot{C}_6 + \dot{C}_{18} + \dot{Z}_{\mathrm{evap}} = \dot{C}_7 + \dot{C}_{19}$	$\frac{\dot{C}_6}{\mathrm{Ex}_6} = \frac{\dot{C}_7}{\mathrm{Ex}_7}$	$c_6 = c_7$
ORCT	$\dot{C}_{19} + \dot{Z}_{ORCT} = \dot{C}_{20} + \dot{C}_{ORCT}$	$\frac{\dot{C}_{19}}{\mathrm{Ex}_{19}} = \frac{\dot{C}_{20}}{\mathrm{Ex}_{20}}$	$c_{19} = c_{20}$
HE	$\dot{C}_{20} + \dot{C}_{17} + \dot{Z}_{\mathrm{OHE}} = \dot{C}_{21} + \dot{C}_{18}$	$\frac{\dot{C}_{20}}{\mathrm{Ex}_{20}} = \frac{\dot{C}_{21}}{\mathrm{Ex}_{21}}$	$c_{20} = c_{21}$
Condenser 2	$\dot{C}_{21} + \dot{C}_{24} + \dot{Z}_{cond2} = \dot{C}_{22} + \dot{C}_{23}$	$\frac{\dot{C}_{21}}{\mathrm{Ex}_{21}} = \frac{\dot{C}_{22}}{\mathrm{Ex}_{22}}$	$c_{21} = c_{22}$
Pump3	$\dot{C}_{22} + \dot{C}_{ORP} + \dot{Z}_{\mathrm{Opump}} = \dot{C}_{17}$	$\frac{\dot{C}_{ORP}}{\dot{W}_{\mathrm{Opump}}} = \frac{\dot{C}_{ORT}}{\dot{W}_{\mathrm{ORT}}}$	

3.8. ASSUMPTIONS AND INPUT PARAMETER TO THE GSO CC

The general assumptions made for the simulation of the combined system are listed as follows:

- All components of the combined system operate under steady-state conditions
- Compositions of air at the inlet of the AC are 79% N_2 and 21% O_2.

- Natural gas is completely oxidized in the CC.
- Ideal gas principles apply to the exhaust gases.
- The CC is insulated completely.

The input data for the GSO CC analysis is recorded in Table 3.3.

Table 3.3 Operation condition used for the GSO CC

Parameter	**Value**
Compression ratio	12
Mass flow rate of fuel (kg/s)	2.4
Mass flow rate of exhaust gases (kg/s)	145
Exhaust gases temperature (K)	500
Ambient temperature (K)	288
Boiler pressure (bar)	100
Condenser pressure (bar)	0.5
Steam turbine inlet temperature (K)	750
Turbine efficiency (%)	90
Compressor efficiency (%)	86
Pump efficiency (%)	85

3.9. COMBINED SYSTEM INTEGRATION IN EES

The EES program is used in the simulation of the GSO CC. The program offers integral solutions, optimization, and graphing. The mass balance, energy balance, and exergy balance analysis of each component is done by using the EES program. In addition, different investigations were completed using EES to find the effect of the input parameters on the GSO CC, such as net work, thermal efficiency, exergy efficiency, and energy cost. Figure 3.2 presents a flow chart for the EES programming based on mathematical modelling of the GSO CC.

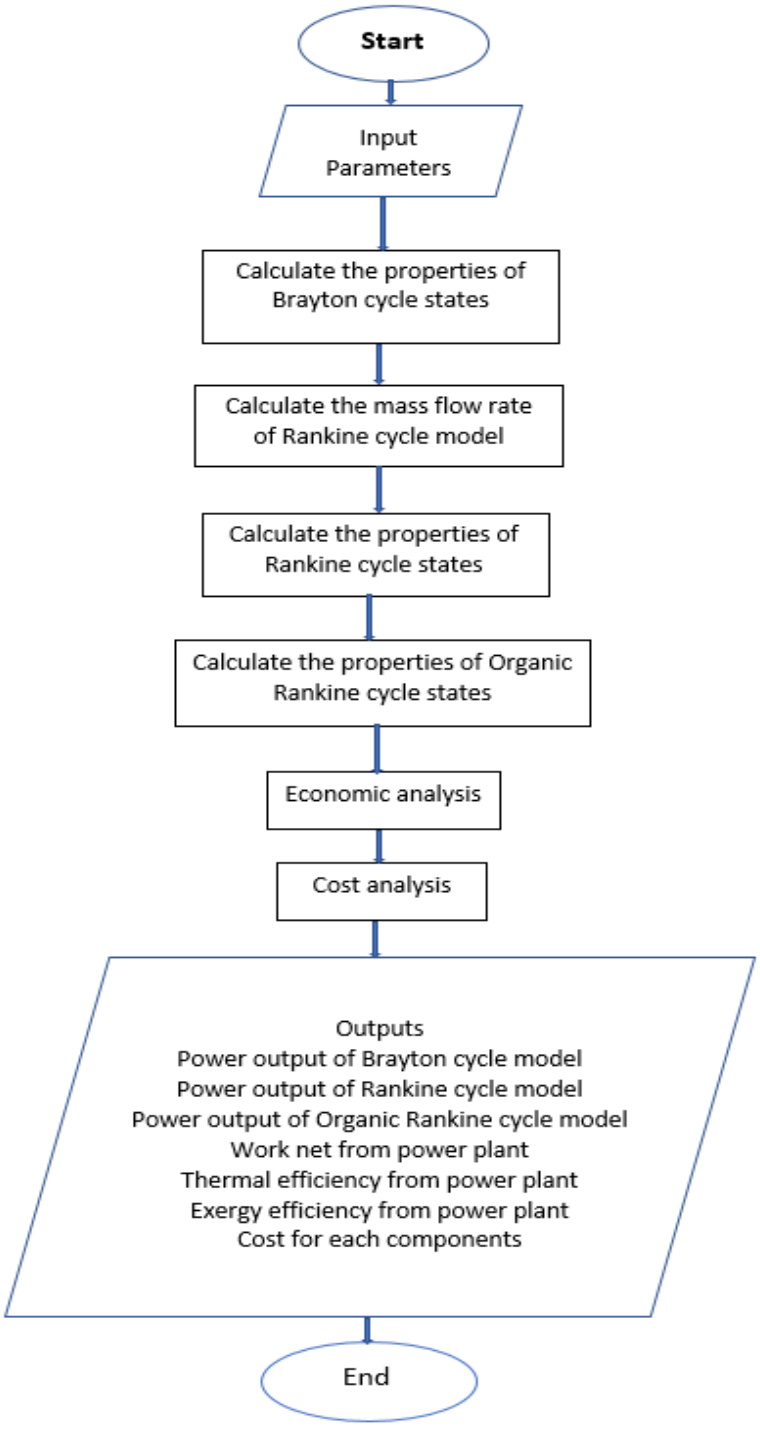

Figure 3.2. Flow chart of the GSO CC

PART 4

RESULTS AND DISCUSSION

This section describes the outcomes of thermodynamics, economic modelling, and the impact of different design factors on the performance of the GSO CC cycle. The suggested heat and power combined cycle system of this research consists of four 160 MW gas turbine cycles with exhaust gases directed into a single-pressure heat recovery steam generator (HRSG) to generate heat. The HRSG receives the water, which exits as superheated vapour. The superheated vapour is introduced into the ST to create additional electricity. Ultimately, a bottoming cycle of the ORC is added to boost system efficiency and maximize the benefit of heat losses, in which the gases ejected from the HRSG are sent to the ORC evaporator. The essential input parameters of the GSO CC cycles are presented in Table 4.2. Table 4.3 details the suggested model's thermodynamic parameters, including each state's mass, enthalpy, entropy, and exergy flow rates.

Table 4.1. Validation of the Brayton cycle model.

Parameter	**Standard**	**Present Model**
Ambient pressure (bar)	1.013	1.013
Ambient temperature (K)	288	288
Pressure ratio	12.1	12.1
Exhaust Flow (kg/s)	145	145.5
Power output (MW)	42.1	41.85
Thermal efficiency	-	29.13

Table 4.2. Operation condition used for the GSO CC model

	Parameter	Value
GT cycle	Compression ratio	11
	Air mass flow rate (kg/s)	142.6*4
	GTIT (°C)	1177
	Ambient temperature (°C)	27
	LHV of fuel ((kJ/kg)	50056
	η_{AC} (%)	84
	η_{GT} (%)	88
	η_{CC} (%)	99.5
RC cycle	ST inlet pressure (bar)	100
	Condenser Temperature (°C)	50
	η_{ST} (%)	90
	η_{Pump} (%)	80
	Effectiveness of HRSG (%)	70
ORC cycle	OST inlet pressure (kPa)	800
	Condenser pressure (bar)	1.2
	Effectiveness of evaporator (%)	70
	Working fluid	R123

Table 4.3. Properties for each state for the GSO CC model at the optimum condition.

State	m (kg/s)	Pressure (kPa)	Temperature (K)	Entropy (kJ/kg. K)	Enthalpy (KJ/kg)	Exergy (MW)
1	498.4	101.3	300	233.6	5.762	0
2	498.4	1226	679.2	627.8	5.886	203.7
3	11.2	101.3	288	−4,672	11.53	518.2
4	509.6	1,165	1450	235.2	8.164	508.8
5	509.6	107.7	919.8	−425.5	8.3	200.72
6	509.6	104.5	500	−904	7.617	41.52
7	509.6	101.3	400	−1,012	7.386	19.4
8	67.56	10,133	445.7	735.5	2.055	11.77
9	67.56	9,829	869.8	3,619	6.904	140.5
10	54.04	12.26	323	2,339	7.298	36.89
11	54.04	12.26	323	208.7	0.7019	2.889
12	54.04	100	323	208.8	0.702	2.893
13	13.51	100	372.8	2617	7.203	13.36
14	67.56	100	372.8	690.4	2.035	9.136
15	637.1	100	300	2,028	7.082	0
16	637.1	100	310	2,781	9.551	7.854
17	177.2	800	306.4	235	1.119	0.1125
18	177.2	800	359.6	292.9	1.292	1.222
19	177.2	800	480	540	1.92	11.86
20	177.2	121.6	428.4	499.3	1.931	4.088
21	177.2	121.6	306.1	402.8	1.669	0.8161
22	177.2	121.6	306.1	234.4	1.119	0.02848
23	39.62	100	300	2,028	7.082	0
24	39.62	100	305	2,404	8.326	0.1238

4.1. ENERGY ANALYSIS RESULTS

Table 4.4 presents the findings of an energy analysis performed on the components of the GSO CC model under the input parameters listed in Table 4.2. The $\dot{W}_{net}$ of the BC model is 167.3 MW, with First Law efficiency (η_I) of 28.74%, and Second Law efficiency (η_{II}) of 27.74%. The RC/ORC model generates 258.2 MW of power by adding RC and ORC cycles. Therefore, the η_I of the RC/ORC cycle increases to 44.37%, and η_{II} increases to 42.84%.

Table 4.4. Performance of the GSO CC model

	BC model	**ORC model**
Net output power	167.3	258.2
Overall exergy efficiency	27.75	42.84
Overall thermal efficiency	28.74	44.37

4.2. EXERGY ANALYSIS RESULTS

As shown in Table 4.5, the total exergy input and exergy destruction for the RC/ORC model are illustrated. The total exergy destruction for all components is approximately 315.3 MW, accounting for 52.31% of the total exergy input to the GT-RC/ORC. Therefore, the valuable work of the GSO CC is 258.2 MW, and its percentage is almost 42.84%. The remaining part of the exergy is released with the exhaust gases to the surrounding environment, and its percentage is nearly 4.85%.

Table 4.5. Exergy input, output, and losses of the model

Exergy	**Values (MW)**	**Percentage (%)**
Input	602.7	100%
Output (network)	258.2	42.84%
Exergy destruction	315.3	52.31%
Exergy losses	29.2	4.85%
Total	602.7	100%

The exergy analysis findings for the RC/ORC system components under ideal conditions are shown in Table 4.6. This table demonstrates that the combustion chambers are where the greatest exergy is lost due to the highly irreversible nature of the combustion process (approx. 57.3%). The HRSG and condenser 1 have the second

and third ranks, respectively, whereas pump 1 experiences the most negligible exergy loss (0.0004%). According to Table 4.6, the highest exergy efficiency is associated with the gas turbine (94.2%).

Table 4.6. Exergy analysis for each component of the (GSO CC) model

Component	$\dot{E}_{input}$ (MW)	$\dot{E}_{output}$ (MW)	$\dot{E}_{destruction}$ (MW)	$\dot{E}_{destruction}$ (%)	Exergy efficiency (%)
AC	224.8	203.7	21.17	6.9	90.6
CC	784.8	608.7	176.1	57.3	77.6
GT	408	384.3	23.73	7.7	94.2
HRSG	159.2	128.8	30.39	9.88	80.9
ST	90.3	82.69	7.6	2.5	91.85
Condenser 1	34	7.85	26.16	8.5	23.1
Deaerator	16.25	9.14	7.12	2.31	56.22
Pump 1	0.006	0.005	0.001	0.0004	81.4
Pump 2	3.05	2.63	0.411	0.134	86.5
ORB	22.14	10.63	11.5	3.74	48
ORT	7.77	7.21	0.55	0.18	92.86
HE	3.27	1.11	2.16	0.7	34
Condenser 2	0.79	0.124	0.66	0.22	15.72
ORP	0.104	0.084	0.02	0.0066	80.6

4.3. EXERGO-ECONOMIC ANALYSIS RESULTS

Exergo-economic analysis is a valuable method for assessing the performance of a thermal system. Table 4.7 shows the cost rates and the cost rates per exergy for each stream in the GSO CC system. The best cost rate is shown in this table for fuel entering and exhaust gases leaving the combustion chamber. The findings of the exergo-economic study for the GSO CC system are shown in Table 4.8. The results indicate that the combustion chamber and steam generator had the highest $\dot{Z}_K + \dot{C}_D$ values, correspondingly. It is clear that condensers have a more considerable relative cost difference than other components because they are less efficient. Evaluating the exergo-economic factor demonstrates that 63% of this cost is attributable to the cost of exergy destruction, whereas only 37% is attributable to investment costs.

Table 4.9 shows the energy cost analysis of the GSO CC system. These findings reveal that the cost of the power produced by the BC is $370.50/h, and the cost of the energy produced by the GSO CC system is $2,470.40/h. The table also shows how each megawatt produced from the GSO CC system costs $9.03, whereas it is $8.24 for the ORC.

Table 4.7. Cost rates and cost rates per unit of exergy of streams in the GSO CC system

State	$\dot{C}$ ($/h)	c ($/GJ)
1	0	0
2	16,522	22.53
3	26,035	12
4	42,578	18.9
5	14,284	18.9
6	2,873	18.9
7	1,364	18.9
8	1,931	43.72
9	13,475	25.46
10	3,496	25.46
11	273.3	25.46
12	273.9	25.48
13	1,269	25.46
14	1,599	46.83
15	0	0
16	3,225	99.85
17	26.12	64.34
18	617.2	140
19	2,141	50.07
20	738.4	50.07
21	147.4	50.07
22	5.144	50.07
23	0	0
24	147.2	329.5

Table 4.8. Exergo-economic results of components of the GSO CC system.

Component	c_f ($/GJ)	c_p ($/GJ)	$\dot{C}_D$ ($/h)	$\dot{Z}_K$ ($/h)	$\dot{Z}_K + \dot{C}_D$ ($/h)	r (%)	f (%)
AC	20.41	22.27	120	190.4	310.4	9.12	61.33
CC	14.66	18.9	735.8	20.1	755.9	28.94	2.65
GT	18.9	20.18	124.2	187.9	312.1	6.75	60.22
HRSG	18.9	23.8	172.9	133	305.9	25.98	43.46
ST	25.46	28.65	56.56	268	324.5	12.55	82.75
Condenser 1	25.46	99.85	185.3	1.5	186.8	292.2	0.82
Deaerator	25.46	46.83	51.94	56.46	108.4	83.91	52.07
Pump 1	28.65	35.99	0.0091	0.014	0.0236	25.95	61.18
Pump 2	28.65	33.12	3.439	0.074	3.513	15.58	2.1
ORB	18.9	39.73	60.53	14.5	75.02	110.2	19.31
ORT	50.07	55.28	7.728	35.65	43.38	10.42	82.19
HE	50.07	147.7	30.14	0.08	30.22	195	0.254
Condenser 2	50.07	329.5	9.251	4.9	14.15	558	34.62
ORP	55.28	69.18	0.311	0.181	0.492	25.13	36.82
Total system	-	-	1,558.0	912.4	2,470.4	-	-

Table 4.9. Energy cost analysis of the GSO CC.

	BC model	GT-ORC model
Total cost ($/h)	1,378	2,470.7
Electricity cost ($/MW)	8.24	9.03

4.4. PARAMETRIC STUDY RESULTS

The effects of changing pressure ratio (Pr), compressor isentropic efficiency (η_{AC}), gas turbine isentropic efficiency (η_{GT}), gas turbine inlet temperature (GTIT), boiler pressure (P_{boiler}), condenser temperature ($T_{condenser}$), and ambient temperature (T_{amb}) on the performance and cost of the GSO CC system are analyzed here.

Figures 4.1 and 4.2 present the impact of the pressure ratio (Pr) on the GSO CC system's performance and cost. The findings demonstrate that $\dot{W}_{BC}$ increases with an increase in Pr until it reaches a maximum point and then decreases with further increases in Pr. At high values of Pr, the power consumed by the compressors increases and affects $\dot{W}_{BC}$ negatively. The maximum $\dot{W}_{BC}$ was obtained at 10 bar (162 MW). The curves also illustrate that $\dot{W}_{net}$ for the GSO CC system decreases with an increase in Pr. At the lower value of Pr, the exhaust temperature from the BC is very high and positively affects $\dot{W}_{RC}$ and $\dot{W}_{ORC}$. The findings reveal that when Pr increases from 4 to 16 bar, $\dot{W}_{net}$ decreases from 277.6 MW to 239 MW for the GSO CC system.

Figure 4.2 reveals the effect of Pr on the efficiencies and cost of the GSO CC system. The GSO CC system's efficiencies and cost improve with a rise in Pr until it peaks and then declines with additional increases in Pr. At high values of Pr, $\dot{W}_{net}$ decreases and negatively affects the efficiencies of the GSO CC system. The maximum η_{energy} and η_{exergy} were obtained at 13 bar (43.89% and 42.38%, respectively). The results also showed that the lower GSO CC system cost was obtained at lower Pr. For the GSO CC system, the lowest $\dot{C}_{electricity}$ is obtained at 7.5 bar ($7.70/MWh), and then $\dot{C}_{electricity}$ jumps to $9.33/MWh at 16 bar.

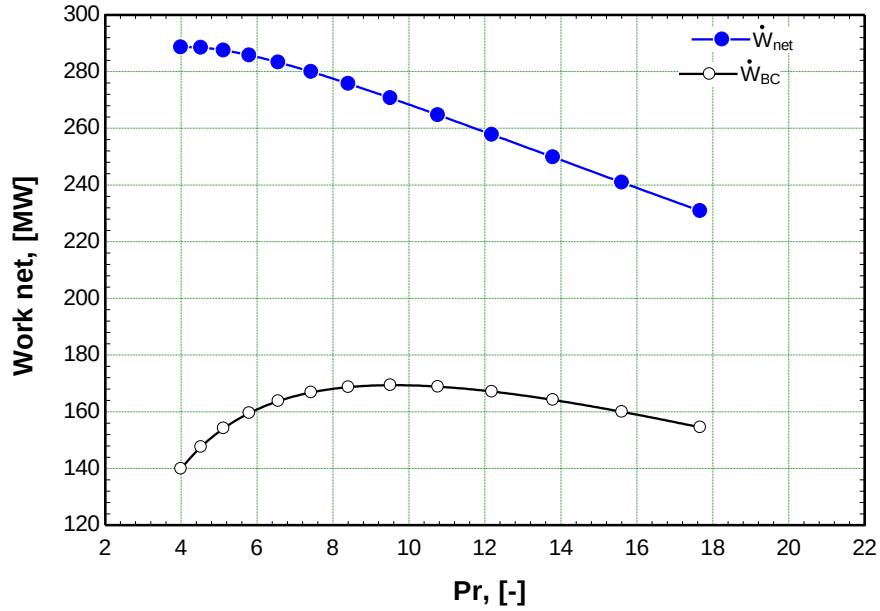

Figure 4.1. Variation of $\dot{W}_{net}$ with pressure ratio (Pr).

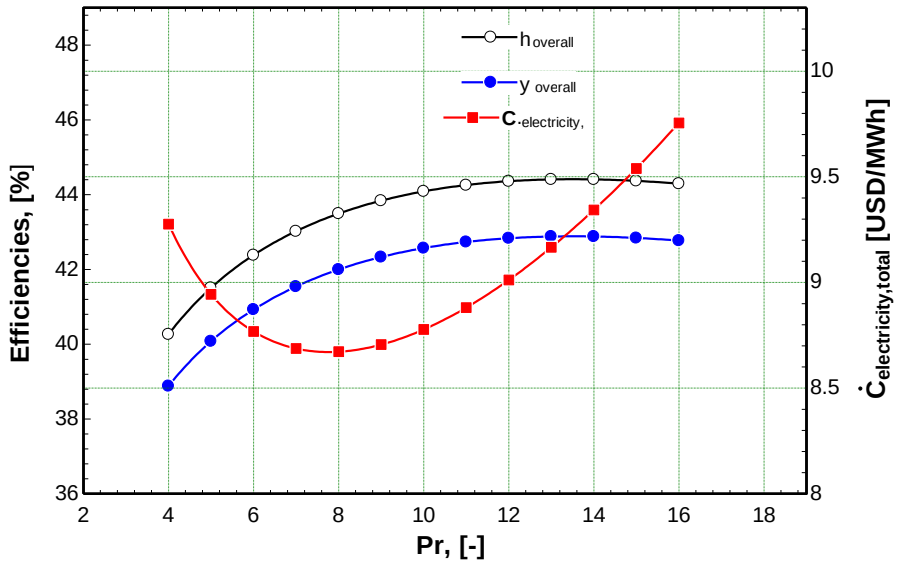

Figure 4.2. Variation of η_{energy}, η_{exergy}, and $\dot{C}_{electricity}$ with pressure ratio (Pr)

4.5. STUDYING THE EFFECT OF COMPRESSOR ISENTROPIC EFFICIENCY

The influence of air compressor isentropic efficiency (η_{AC}) on system performance and total cost rate is shown in Figures 4.3 and 4.4. The figures revealed that a rise in η_{AC} results in an increase in both $\dot{W}_{net}$ and the efficiencies of the GSO CC system. If the airflow rates remain constant, increasing the η_{AC} will reduce the power consumption of the compressor, increasing the gas turbine's power production. Figure 4.3 shows that a change in η_{AC} from 70% to approximately 88% increases total $\dot{W}_{net}$ from 215.6 MW to 275 MW. Figure 4.4 shows that when η_{AC} was raised, the First- and Second-Law efficiencies of the cycle would improve. The results indicate that increasing η_{AC} is needed in order to attain greater efficiency. However, this is not economical. Based on these findings, increasing η_{AC} from 70% to approximately 84% results in a lower cycle's overall cost. However, further raising η_{AC} to beyond 84% superfast the cycle's overall cost.

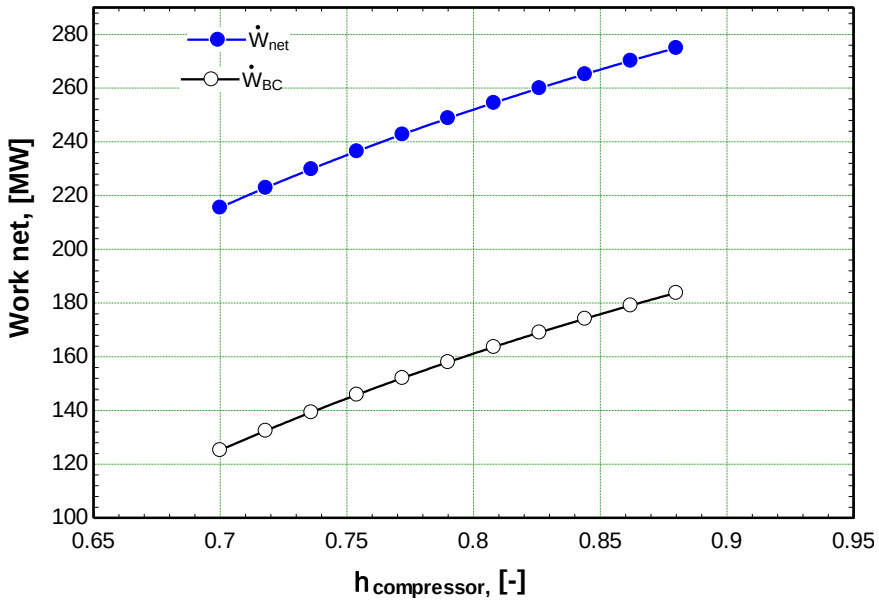

Figure 4.3. Variation of $\dot{W}_{net}$ with η_{AC}

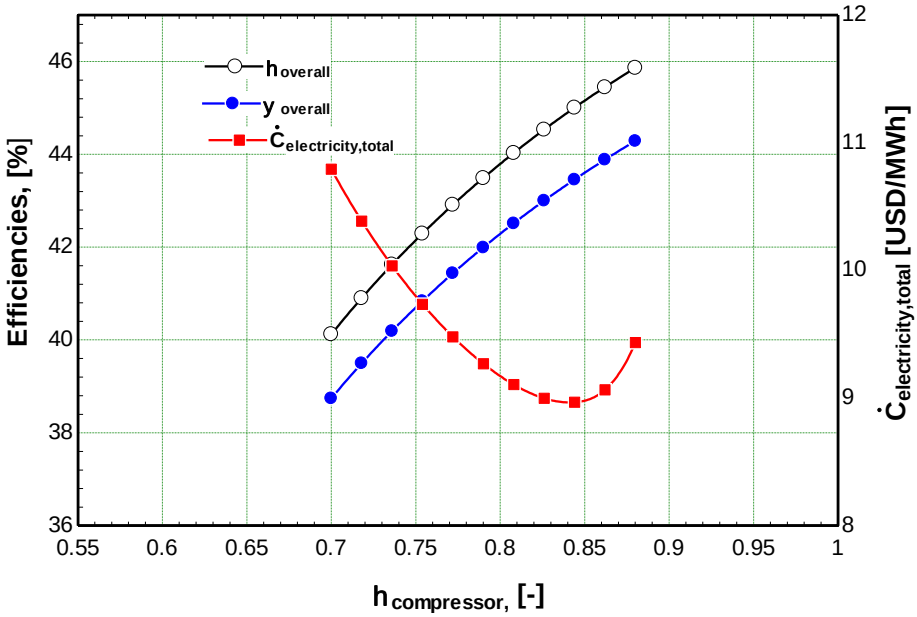

Figure 4.4. Variation of η_{energy}, η_{exergy}, and $\dot{C}_{electricity}$ with η_{AC}

4.6. STUDYING THE EFFECT OF TURBINE ISENTROPIC EFFICIENCY

Figures 4.5 and 4.6 show how the isentropic efficiency of gas turbines (η_{GT}) affects the performance of the GSO CC system and the rate of total costs. $\dot{W}_{net}$ and the efficiencies of the suggested system improved by increasing η_{GT}. By maximizing η_{GT}, the exergy destruction rate of the system was reduced and hence boosted the overall net and efficiencies of the proposed system. Figure 4.5 presents that when η_{GT} increases from 0.7 to 0.9, $\dot{W}_{net}$ improves from 212.1 MW to 270 MW for the system. Additionally, η_{energy} of the GSO CC system increases from 36.45% to 46.75 % and η_{exergy} rises from 35.2% to 44.78%, as seen in Figure 4.6. By increasing η_{GT}, the overall cost rate of the system initially drops and subsequently rises. As the gas turbine's isentropic efficiency rises, the investment cost rate of the ORC components increases by growing the mass flow rate of the working fluid. As a result of these variations, the overall cost rate will initially fall and then rise. With an increase in η_{GT}, $\dot{C}_{electricity}$ drops significantly from \$14.40/MWh until it reaches a minimum value of \$9.03/MWh at η_{GT} of 86%, and then it increases to \$9.24/MWh at η_{GT} of 90%.

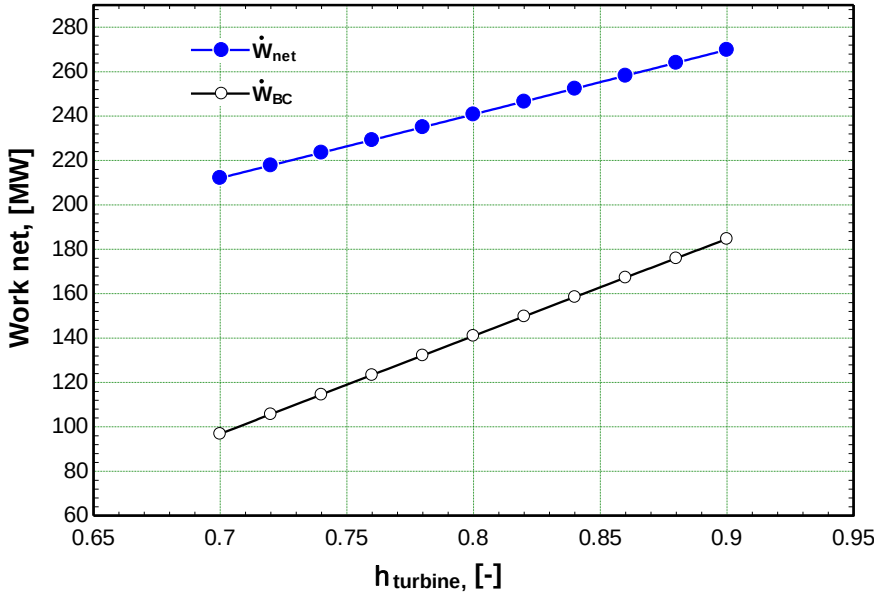

Figure 4.5. Variation of $\dot{W}_{net}$ with η_{GT}

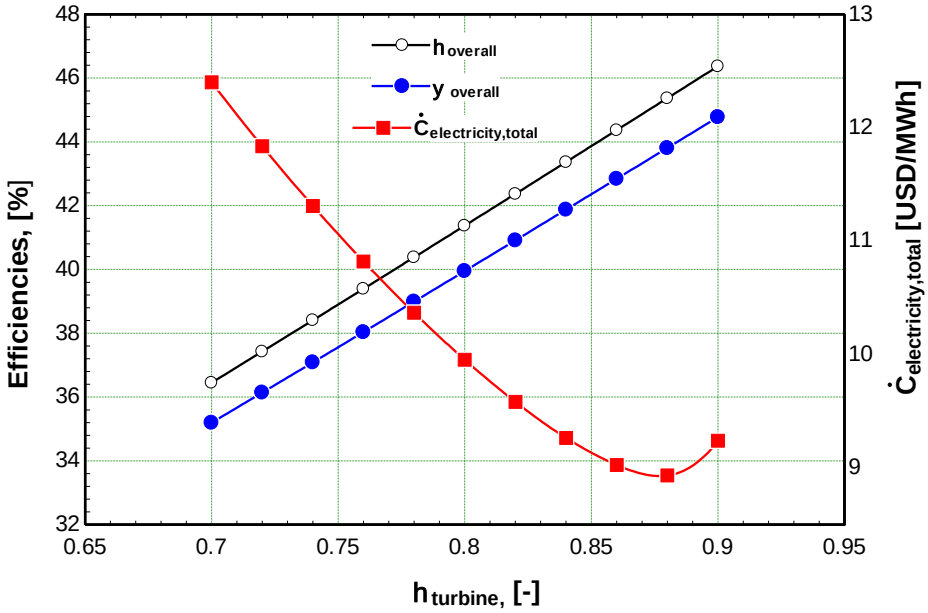

Figure 4.6. Variation of η_{energy}, η_{exergy}, and $\dot{C}_{electricity}$ with η_{GT}

4.7. STUDYING THE EFFECT OF GAS TURBINE INLET TEMPERATURE

Figures 4.7 and 4.8 show the variation of $\dot{W}_{net}$, η_{energy}, η_{exergy}, and $\dot{C}_{electricity}$ with GTIT. These figures demonstrate that a change in GTIT has a substantial effect on the values of $\dot{W}_{net}$, η_{energy}, η_{exergy}, and $\dot{C}_{electricity}$. With a rise in GTIT, the temperature of the exhaust gases leaving the gas turbine rises, increasing the thermal energy transferred from the exhaust gases in the HRSG to the RC. This produces an increase in the $\dot{W}_{net}$ of the RC

and ORC. Additionally, when the GTIT increases, the overall system becomes more efficient. Therefore, an increase in the GTIT from 1,200 K to 1,525 K dramatically increases $\dot{W}_{net}$ from 133.2 MW to 282.6 MW, and η_{energy} improves substantially from 36.74% to 45.29%, while η_{exergy} increases from 35.74% to 43.73%. Figure 4.8 also illustrates how a change in the GTIT affects the entire cost of the cycle. $\dot{C}_{electricity}$ first declines drastically when the GTIT rises but subsequently considerably increases at higher GTIT levels. $\dot{C}_{electricity}$ becomes minimal at a GTIT of 1,475 K, leading to minimum $\dot{C}_{electricity}$ at \$8.24/MWh. With an increase in the GTIT, $\dot{C}_{electricity}$ reduces significantly from \$14.86/MWh until it falls to a minimum value of \$8.24/MWh at a GTIT of 1,475 K, and then increases to \$8.86/MWh at a GTIT of 1,525 K.

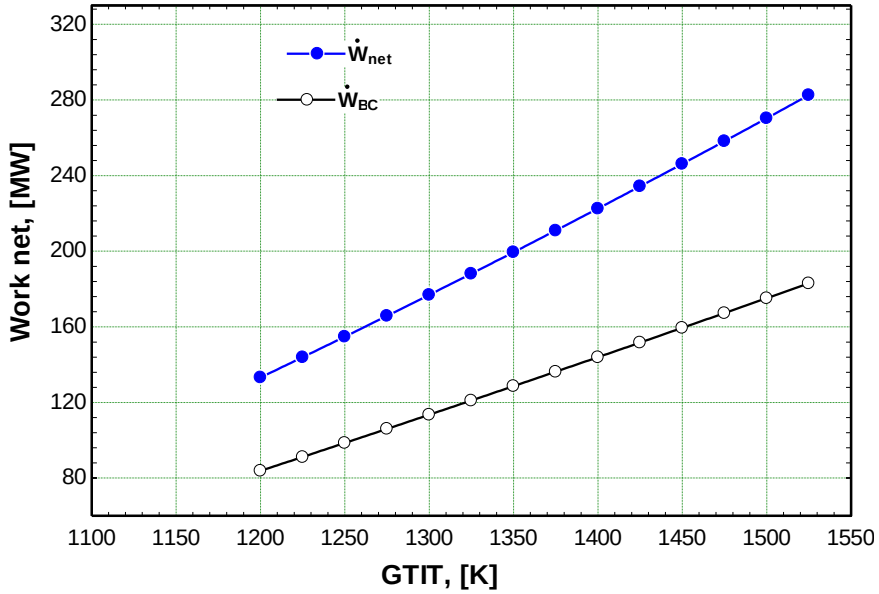

Figure 4.7. Variation of $\dot{W}_{net}$ with GTIT

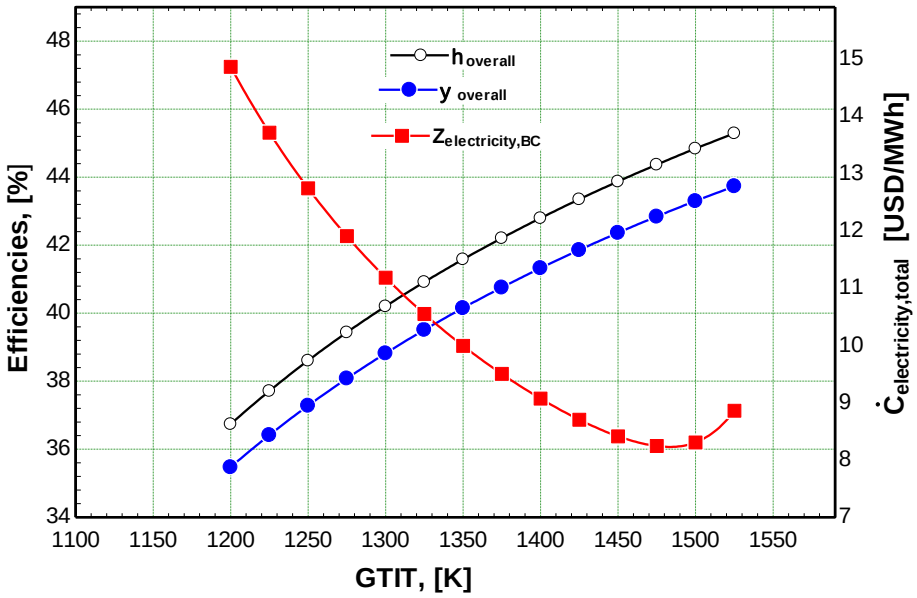

Figure 4.8. Variation of η_{energy}, η_{exergy}, and $\dot{C}_{electricity}$ with GTIT

4.8. STUDYING THE EFFECT OF BOILER PRESSURE

Figures 4.9 and 4.10 show how the boiler pressure (P_{boiler}) affects the performance of the GSO CC system and the rate of total costs. Since the net work of the BC cycle remains constant regardless of the value of P_{boiler}, the net work of the RC improves when P_{boiler} rises due to the higher enthalpy of the water leaving the boiler, as seen in Figure 4.9. Consequently, when P_{boiler} climbs from 75 bar to 130 bar, $\dot{W}_{net}$ for the GSO CC system increases from 256 MW to 260 MW. Likewise, the efficiencies of the GSO CC system also increase at high P_{boiler}. Figure 4.10 shows that as P_{boiler} increases, η_{energy} increases from 44% to 44.68%, and η_{exergy} increases from 42.5% to 43.14%. The graph also shows that when P_{boiler} decreases from 130 bar to 75 bar, $\dot{C}_{electricity}$ rises from \$8.93/MWh to \$9.15/MWh. The decreased power output of the GSO CC system at a lower P_{boiler} is the fundamental cause of the rise in $\dot{C}_{electricity}$.

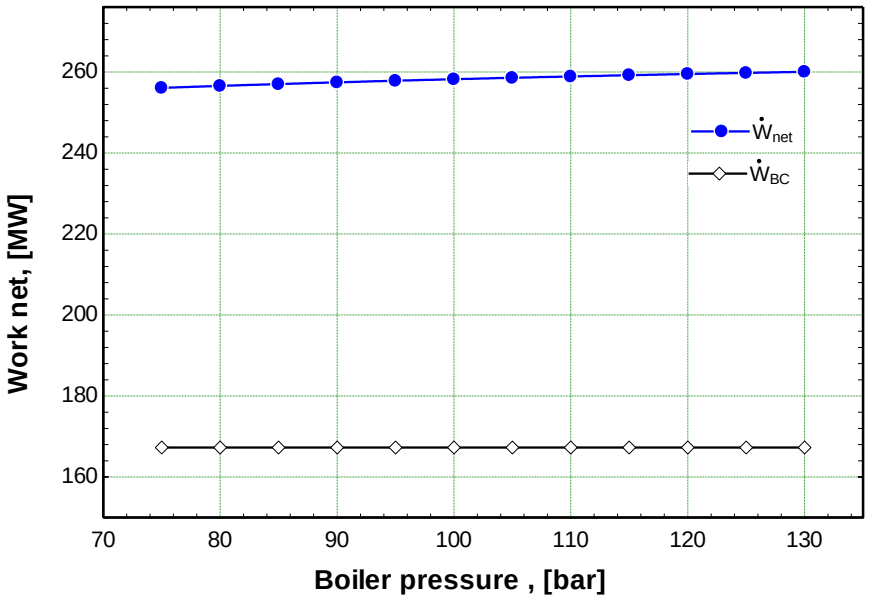

Figure 4.9. Variation of $\dot{W}_{net}$ with boiler pressure

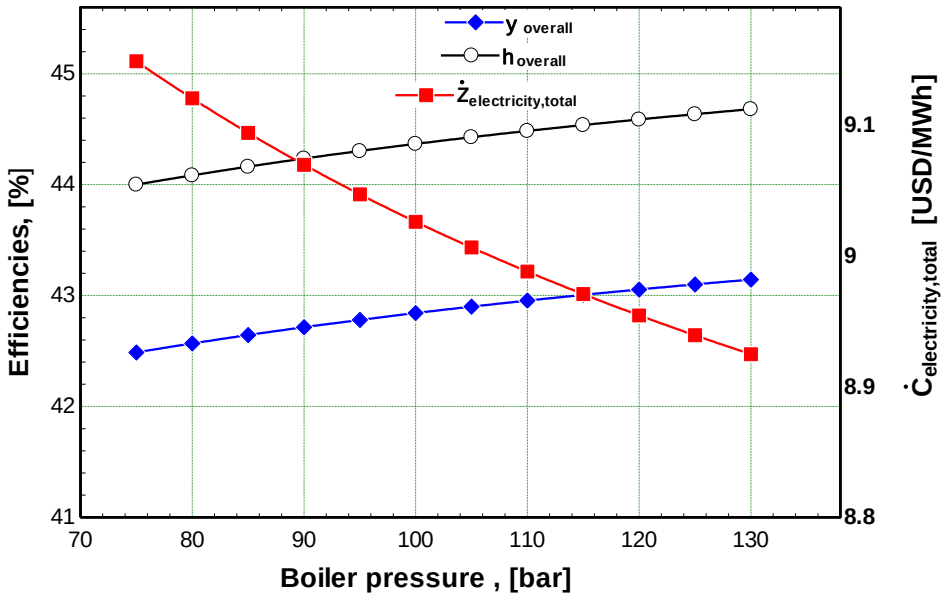

Figure 4.10. Variation of η_{energy}, η_{exergy}, and $\dot{C}_{electricity}$ with boiler pressure

4.9. STUDYING THE EFFECT OF CONDENSER TEMPERATURE

The influence of Rankine cycle condenser temperature ($T_{condenser}$) on system performance and total cost rate is shown in Figures 4.11 and 4.12. The finding demonstrates that when $T_{condenser}$ rises, the RC's power output decreases, limiting $\dot{W}_{net}$, η_{energy}, and η_{exergy} of the GSO CC system. $\dot{W}_{net}$ drops from 263.4 MW to 251.3 MW (approximately 12.1 MW) when $T_{condenser}$ increases from 303 K to 348 K, as seen in

Figure 4.11. Figure 4.12 also shows how η_{energy} falls from 45.27 to 43.19%, while η_{exergy} decreases from 43.71% to 41.7%. The results also show that the diminishment in the $\dot{W}_{net}$ of the GSO CC leads to an increase in $\dot{C}_{electricity}$ at high $T_{condenser}$. $\dot{C}_{electricity}$ increases from \$8.70/MWh to \$9.524/MWh with variations of $T_{condenser}$ between 303 K and 348 K.

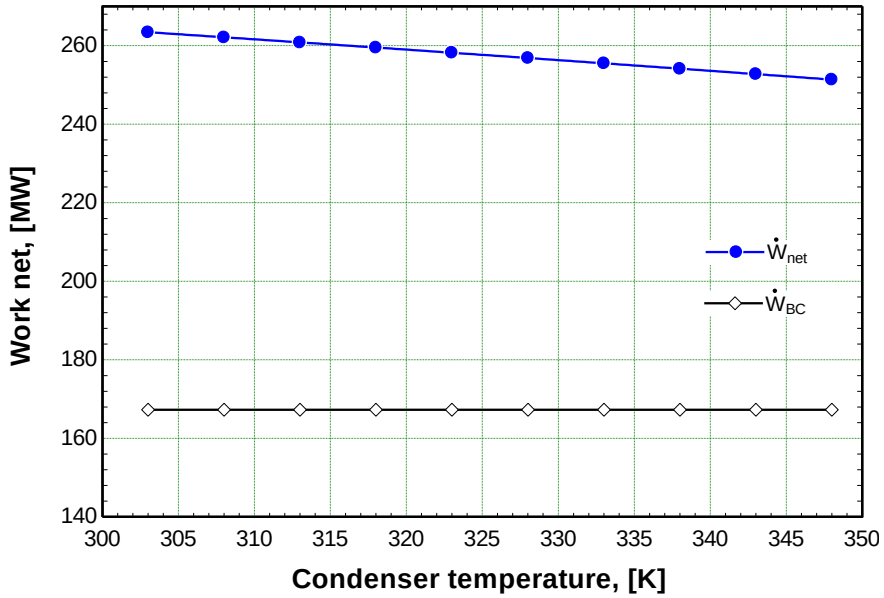

Figure 4.11. Variation of $\dot{W}_{net}$ with condenser temperature.

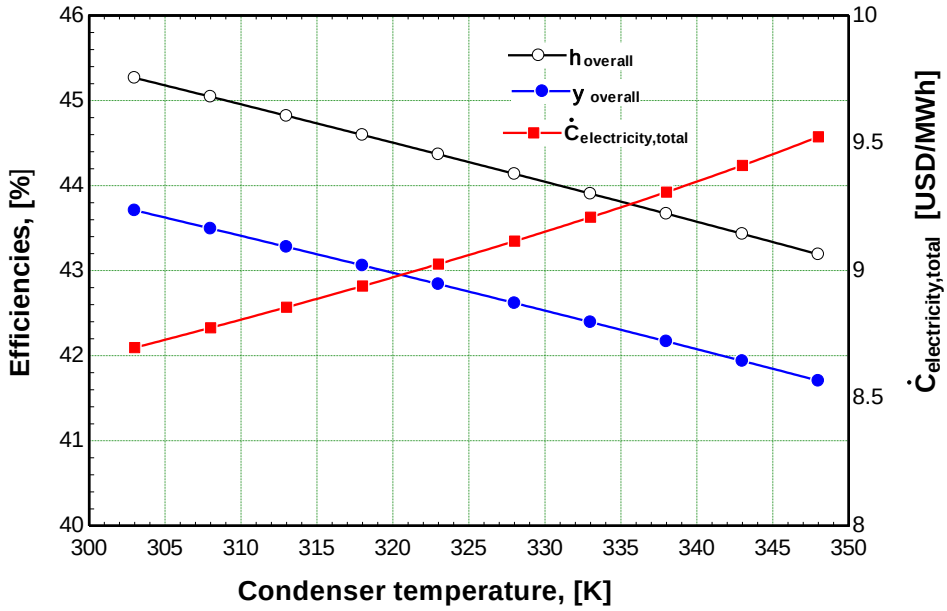

Figure 4.12. Variation of η_{energy}, η_{exergy}, and $\dot{C}_{electricity}$ with condenser temperature.

PART 5

CONCLUSION

This research was undertaken on the Baghdad-based Taji gas station in the context of integrating the plant with the Rankine cycle and organic Rankine cycle to verify waste heat recovery to produce extra electricity and reduce environmental emissions. Using this work as a foundation is advantageous, and it may be used to generate additional energy in the future. The key conclusions of the research may be stated as follows:

- The $\dot{W}_{net}$ of the BC model is 167.3 MW, with η_{energy} of 28.74%, and η_{exergy} of 27.74%. The GSO CC model increases $\dot{W}_{net}$ to 258.2 MW of power by adding RC and ORC cycles. The, the η_{energy} of the GSO CC cycle improves to 44.37%, and η_{exergy} to 42.84%.
- The total exergy destruction for all components is approximately 315.3 MW, accounting for 52.31% of the total exergy input to the GSO CC. Therefore, the valuable work of the GSO CC is 258.2 MW, and its percentage is almost 42.84%.
- The cost of the energy produced by the GSO CC system is $2,470.4/h (each megawatt produced from by GSO CC system costs $9.03).
- The exergo-economic factor demonstrates that 63% of the cost is attributable to the cost of exergy destruction, whereas only 37% is attributable to investment costs.
- $\dot{W}_{net}$ for the GSO CC system decreases with an increase in Pr. At the lower value of Pr, the exhaust temperature from BC is very high and affected positively by $\dot{W}_{RC}$ and $\dot{W}_{ORC}$.
- The efficiencies of the GSO CC system and cost improve with a rise in Pr until it arrives at a peak and then declines with additional increases in Pr.
- The efficiencies of the GSO CC system grow with the pressure ratio up to a maximum, beyond which they decrease with further increases in Pr.

- With the change in η_{AC} from 70% to approximately 88%, $\dot{W}_{net}$ increases from 215.6 MW to 275 MW in the GSO CC system.
- Increasing η_{AC} from 70% to approximately 84% results in a lower cycle's overall cost. However, further increasing η_{AC} beyond 84% increases the cycle's overall cost.
- When η_{GT} increases from 0.7 to 0.9, $\dot{W}_{net}$ increases from 212.1 MW to 270 MW for the system. Moreover, η_{energy} of the GSO CC system increases from 36.45% to 46.75% and η_{exergy} rises from 35.2% to 44.78%.
- With an increase in η_{GT}, $\dot{C}_{electricity}$ drops significantly from \$14.40/MWh until it reaches a minimum value of \$9.03/MWh at η_{GT} of 86%, and then increases to \$9.24/MWh at η_{GT} of 90%.
- Increasing GTIT from 1,200 K to 1,525 K dramatically increases $\dot{W}_{net}$ from 133.2 MW to 282.6 MW, and η_{energy} increases substantially from 36.74% to 45.29% while η_{exergy} increases from 35.74% to 43.73%.
- $\dot{C}_{electricity}$ becomes minimal at GTIT of 1,475 K, leading to a minimum cost of \$8.24/MWh.
- When P_{boiler} climbs from 75 to 130 bar, the $\dot{W}_{net}$ for the GSO CC system increases from 256 MW to 260 MW, and $\dot{C}_{electricity}$ drops from \$9.15/MWh to \$8.93/MWh.
- When $T_{condenser}$ rises, the RC's power output decreases, limiting the $\dot{W}_{net}$, η_{energy}, and η_{exergy} of the GSO CC system. The $\dot{W}_{net}$ drops from 263.4 MW to 251.3 MW (approximately 12.1 MW) when $T_{condenser}$ increases from 303 K to 348 K.
- The reduction in the $\dot{W}_{net}$ of GSO CC leads to an increase in $\dot{C}_{electricity}$ at high $T_{condenser}$. $\dot{C}_{electricity}$ increases from \$8.70/MWh to \$9.524/MWh with a variety of $T_{condenser}$ between 303 K and 348 K.

REFERENCES

1. Horlock, J. H., "Combined heat and power", ***Web.***, United Sta: (1987).

2. Olesen, J. F. and Shaker, H. R., "Predictive maintenance for pump systems and thermal power plants: State-of-the-art review, trends and challenges", ***Sensors (Switzerland)***, 20 (8): (2020).

3. Rinne, S. and Syri, S., "Heat pumps versus combined heat and power production as CO2 reduction measures in Finland", ***Energy***, 57: 308–318 (2013).

4. Jouhara, H., Khordehgah, N., Almahmoud, S., Delpech, B., Chauhan, A., and Tassou, S. A., "Waste heat recovery technologies and applications", ***Thermal Science And Engineering Progress***, 6 (January): 268–289 (2018).

5. Thekdi, A. and Nimbalkar, S. U., "Industrial Waste Heat Recovery : Potential Applications, Available Technologies and Crosscutting R&D Opportunities", Oak Ridge National Laboratory, 82 (2015).

6. Cheng, K., Qin, J., Dang, C., Lv, C., Zhang, S., and Bao, W., "Thermodynamic analysis for high-power electricity generation systems based on closed-Brayton-cycle with finite cold source on hypersonic vehicles", ***International Journal Of Hydrogen Energy***, 43 (31): 14762–14774 (2018).

7. Zhu, D. and Zheng, X., "Potential for energy and emissions of asymmetric twin-scroll turbocharged diesel engines combining inverse Brayton cycle system", ***Energy***, 179: 581–592 (2019).

8. Shalan, H., Hassan, M., and Bahgat, A., "Comparative Study on Modeling of Gas Turbines in Combined Cycle Power Plants", ***Proceedings Of The 14th International Middle East Power Systems Conference (MEPCON'10)***, (April): 970–976 (2010).

9. Kunitomi, K., Kurita, A., Tada, Y., Member, A., Ihara, S., Price, W. W., Richardson, L. M., and Smith, G., "Modeling Combined-Cycle Power Plant for Simulation of Frequency Excursions", 18 (2): 724–729 (2003).

10. Rahman, M. M., Ibrahim, T. K., and Abdalla, A. N., "Thermodynamic performance analysis of gas-turbine power-plant", ***International Journal Of Physical Sciences***, 6 (14): 3539–3550 (2011).

11. Cha, S. H., Na, S. I., Lee, Y. H., and Kim, M. S., "Thermodynamic analysis of a gas turbine inlet air cooling and recovering system in gas turbine and CO2 combined cycle using cold energy from LNG terminal", ***Energy Conversion And Management***, 230: 113802 (2021).

12. Loni, R., Najafi, G., Bellos, E., Rajaee, F., Said, Z., and Mazlan, M., "A review of industrial waste heat recovery system for power generation with Organic Rankine Cycle: Recent challenges and future outlook", ***Journal Of Cleaner Production***, 287: (2021).

13. Xu, Z. Y., Wang, R. Z., and Yang, C., "Perspectives for low-temperature waste heat recovery", ***Energy***, 176: 1037–1043 (2019).

14. Cignitti, S., Andreasen, J. G., Haglind, F., Woodley, J. M., and Abildskov, J., "Integrated working fluid-thermodynamic cycle design of organic Rankine cycle power systems for waste heat recovery", ***Applied Energy***, 203: 442–453 (2017).

15. Akroot, A. and Namli, L., "Performance assessment of an electrolyte-supported and anode-supported planar solid oxide fuel cells hybrid system", ***J Ther Eng***, 7 (7): 1921–1935 (2021).

16. Nuvolari, A., Verspagen, B., Nuvolari, A., Verspagen, B., and Von Tunzelmann, N., "The early diffusion of the steam engine in Britain, 1700–1800: a reappraisal", 5: 291–321 (2011).

17. Cengel, Y. A. and Boles, M. A., "Thermodynamics: An Engineering Approach 8th Edition", McGraw-Hill, (2015).

18. Yunus A Çengel, "Thermodynamics: An Engineering Approach", Angewandte Chemie International Edition, 6(11), 951–952., 2013–2015 (2003).

19. MORAN, M. J. and SHAPIRO, HOWARD N.BOETTNER, D. D. M. B. B., "Fundamentals of Engineering Thermodynamics", WILEY, 14–61 (2020).

20. Liu, Y., Wang, Y., and Huang, D., "Supercritical CO2 Brayton cycle: A state-of-the-art review", ***Energy***, 189: 115900 (2019).

21. Peterson, P. F., "Multiple-reheat Brayton cycles for nuclear power conversion with molten coolants", ***Nuclear Technology***, 144 (3): 279–288 (2003).

22. Syblik, J., Vesely, L., Entler, S., Stepanek, J., and Dostal, V., "Analysis of supercritical CO2 Brayton power cycles in nuclear and fusion energy", ***Fusion Engineering And Design***, 146 (March): 1520–1523 (2019).

23. Zohuri, B., McDaniel, P. J., and De Oliveira, C. R. E., "Advanced nuclear open air-Brayton cycles for highly efficient power conversion", ***Nuclear Technology***, 192 (1): 48–60 (2015).

24. Rahbar, K., Mahmoud, S., Al-Dadah, R. K., Moazami, N., and Mirhadizadeh, S. A., "Review of organic Rankine cycle for small-scale applications", ***Energy Conversion And Management***, 134: 135–155 (2017).

25. Bao, J. and Zhao, L., "A review of working fluid and expander selections for organic Rankine cycle", ***Renewable And Sustainable Energy Reviews***, 24: 325–342 (2013).

26. Mondejar, M. E., Andreasen, J. G., Pierobon, L., Larsen, U., Thern, M., and Haglind, F., "A review of the use of organic Rankine cycle power systems for maritime applications", ***Renewable And Sustainable Energy Reviews***, 91: 126–151 (2018).

27. Tchanche, B. F., Quoilin, S., Declaye, S., Papadakis, G., and Lemort, V., "Economic feasibility study of a small scale organic rankine cycle system in waste heat recovery application", ***ASME 2010 10th Biennial Conference On Engineering Systems Design And Analysis, ESDA2010***, 1 (July): 249–256 (2010).

28. Shalan, H., Hassan, M., and Bahgat, A., "Comparative Study on Modeling of Gas Turbines in Combined Cycle Power Plants", ***Proceedings Of The 14th International Middle East Power Systems Conference (MEPCON'10)***, (January 2010): 970–976 (2010).

29. Bălănescu, D. T. and Homutescu, V. M., "Performance analysis of a gas turbine combined cycle power plant with waste heat recovery in Organic Rankine Cycle", ***Procedia Manufacturing***, 32: 520–528 (2019).

30. Reshaeel, M., Javed, A., Jamil, A., Ali, M., Mahmood, M., and Waqas, A., "Multiparametric optimization of a reheated organic Rankine cycle for waste heat recovery based repowering of a degraded combined cycle gas turbine power plant", ***Energy Conversion And Management***, 254 (January): 115237 (2022).

31. Wang, X. and Duan, L., "Peak regulation performance study of the gas turbine combined cycle based combined heating and power system with gas turbine interstage extraction gas method", ***Energy Conversion And Management***, 269 (August): 116103 (2022).

32. Zhu, S., Ma, Z., Zhang, K., and Deng, K., "Energy and exergy analysis of the combined cycle power plant recovering waste heat from the marine two-stroke engine under design and off-design conditions", ***Energy***, 210: 118558 (2020).

33. Wang, H. X., Lei, B., and Wu, Y. T., "Simulations on organic Rankine cycle with quasi two-stage expander under cross-seasonal ambient conditions", ***Applied Thermal Engineering***, 222 (December 2022): 119939 (2023).

34. Dawo, F., Buhr, J., Schifflechner, C., Wieland, C., and Spliethoff, H., "Experimental assessment of an Organic Rankine Cycle with a partially evaporated working fluid", ***Applied Thermal Engineering***, 221 (January 2022): 119858 (2023).

35. E Elahi, A., Mahmud, T., Alam, M., Hossain, J., and Biswas, B. N., "Exergy analysis of organic Rankine cycle for waste heat recovery using low GWP refrigerants", ***International Journal Of Thermofluids***, 16 (November): 100243 (2022).

36. Xia, X., Liu, Z., Wang, Z., Sun, T., Zhang, H., and Zhang, S., "Thermo-economic-environmental optimization design of dual-loop organic Rankine cycle under fluctuating heat source temperature", ***Energy***, 264 (November 2022): 126144

(2023).

37. Zahedi, R., Aslani, A., Seraji, M. A. N., and Zolfaghari, Z., "Advanced bibliometric analysis on the coupling of energetic dark greenhouse with natural gas combined cycle power plant for CO2 capture", ***Korean Journal Of Chemical Engineering***, 39 (11): 3021–3031 (2022).

38. Atılgan Türkmen, B., "Environmental performance of high-efficiency natural gas combined cycle plant", ***Energy Sources, Part A: Recovery, Utilization And Environmental Effects***, 44 (1): 57–74 (2022).

39. Nourpour, M. and Khoshgoftar Manesh, M. H., "Modeling and 6E Analysis of a Novel Quadruple Combined Cycle with Turbocompressor Gas Station", Journal of Thermal Analysis and Calorimetry, ***Springer International Publishing***, 5165–5197 (2022).

40. Nourpour, M. and Khoshgoftar Manesh, M. H., "Evaluation of novel integrated combined cycle based on gas turbine-SOFC-geothermal-steam and organic Rankine cycles for gas turbo compressor station", ***Energy Conversion And Management***, 252 (August 2021): 115050 (2022).

41. Cihan, E., "Organik Rankine çevrimi ile çalışan atık ısı kaynaklı bir soğutma sisteminin performansının araştırılması", ***Isı Bilimi Ve Tekniği Dergisi***, 34 (1): 101–109 (2014).

42. Wei, D., Lu, X., Lu, Z., and Gu, J., "Performance analysis and optimization of organic Rankine cycle (ORC) for waste heat recovery", ***Energy Conversion And Management***, 48 (4): 1113–1119 (2007).

43. Kaşka, Ö., "Energy and exergy analysis of an organic Rankine for power generation from waste heat recovery in steel industry", ***Energy Conversion And Management***, 77: 108–117 (2014).

44. Mago, P. J., L. Chamra, M., and Somayaji, C., "Performance analysis of different working fluids for use in organic Rankine cycles", ***Journal Of Power And Energy Institution Of Mechanical Engineers***, (2007).

45. Liu, B. T., Chien, K. H., and Wang, C. C., "Effect of working fluids on organic Rankine cycle for waste heat recovery", ***Energy***, 29 (8): 1207–1217 (2004).

46. Roy, J. P., Mishra, M. K., and Misra, A., "Parametric optimization and performance analysis of a waste heat recovery system using Organic Rankine Cycle", ***Energy***, 35 (12): 5049–5062 (2010).

47. Dai, Y., Wang, J., and Gao, L., "Parametric optimization and comparative study of organic Rankine cycle (ORC) for low grade waste heat recovery", ***Energy Conversion And Management***, 50 (3): 576–582 (2009).

48. Wang, E. H., Zhang, H. G., Fan, B. Y., Ouyang, M. G., Zhao, Y., and Mu, Q. H., "Study of working fluid selection of organic Rankine cycle (ORC) for engine waste heat recovery", ***Energy***, 36 (5): 3406–3418 (2011).

49. Zhu, Q., Sun, Z., and Zhou, J., "Performance analysis of organic rankine cycles using different working fluids", ***Thermal Science***, 19 (1): 179–191 (2015).

50. Kumar Tyagi, S. and Chen, J., "Performance evaluation of an irreversible regenerative modified Brayton heat engine based on the thermoeconomic criterion", ***International Journal Of Power And Energy Systems***, 26 (1): 66–74 (2006).

51. Tyagi, S. K., Tyagi, S. K., Chen, J., and Kaushik, S. C., "Optimal criteria based on the ecological function of an irreversible intercooled regenerative modified Brayton cycle", ***International Journal Of Exergy***, 2 (1): 90–107 (2005).

52. Al-Doori, W. H. A. R., "Parametric performance of gas turbine power plant with effect intercooler", ***Modern Applied Science***, 5 (3): 173–184 (2011).

53. Abou Al-Sood, M. M., Matrawy, K. K., and Abdel-Rahim, Y. M., "Optimum Operating Parameters of an Irreversible Gas Turbine Cycle", ***JES. Journal Of Engineering Sciences***, 40 (6): 1695–1714 (2012).

54. Tyagi, S. K., Wang, S. W., Chen, G. M., Han, X. H., and Kaushik, S. C., "Optimal criteria for different parameters of an irreversible regenerative intercooled Brayton cycle under maximum power and maximum ecological COP conditions", ***International Journal Of Ambient Energy***, 27 (1): 37–51 (2006).

55. Zhang, Z., Chen, L., and Sun, F., "Performance optimisation for two classes of combined regenerative Brayton and inverse Brayton cycles", ***International Journal Of Sustainable Energy***, 33 (4): 723–741 (2014).

56. Abadi, M.J., Hooshmand, P., Khezri, B., Radmanesh, A. ., "Investigation of using different fluids for using in gas turbine-Rankine cycle", ***Indian Journal Of Scientific Research***, 1(2), 74–8: (2014).

57. Wang, D., Ling, X., and Peng, H., "Performance analysis of double organic Rankine cycle for discontinuous low temperature waste heat recovery", ***Applied Thermal Engineering***, 48: 63–71 (2012).

58. Hung, T.C., Shai, T.Y., Wang, S. K., "A review of organic Rankine cycles (ORCs) for the recovery of low-grade waste heat", ***Energy***, 661–667: (1997).

59. Song, J., Li, X. song, Ren, X. dong, and Gu, C. wei, "Performance analysis and parametric optimization of supercritical carbon dioxide (S-CO2) cycle with bottoming Organic Rankine Cycle (ORC)", ***Energy***, 143: 406–416 (2018).

60. Chacartegui, R., Sánchez, D., Muñoz, J. M., and Sánchez, T., "Alternative ORC bottoming cycles FOR combined cycle power plants", ***Applied Energy***, 86 (10): 2162–2170 (2009).

61. Lu, X., Zhao, Y., Zhu, J., and Zhang, W., "Optimization and applicability of compound power cycles for enhanced geothermal systems", ***Applied Energy***, 229 (December 2017): 128–141 (2018).

62. Yang, F., Zhang, H., Yu, Z., Wang, E., Meng, F., Liu, H., and Wang, J., "Parametric optimization and heat transfer analysis of a dual loop ORC (organic Rankine cycle) system for CNG engine waste heat recovery", ***Energy***, 118: 753–775 (2017).

63. Zhang, X., Bai, H., Li, N., and Zhang, X., "Power generation by Organic Rankine cycle from low temperature waste heat of metallurgical industry", ***TMS Annual Meeting***, 14-18-Febr (January): 57–64 (2016).

64. Safari, F. and Ataei, A., "Thermodynamic Performance Analysis of Different Organic Rankine Cycles to Generate Power from Renewable Energy Resources.", ***4th International Conference On Emerging Trends In Energy Conservation***, 1 (2): 31–38 (2015).

65. Mohapatra, A. K. and Sanjay, "Thermodynamic assessment of impact of inlet air cooling techniques on gas turbine and combined cycle performance", ***Energy***, 68: 191–203 (2014).

66. Van Wylen, Gordon J.; Sonntag, R. E., "Fundamentals of Thermodynamics: Seventh Edition", John Wiley & Sons, Inc., U.S.A., A472 (2009).

67. Akroot, A. and Nadeesh, A., "Performance Analysis of Hybrid Solid Oxide Fuel Cell-Gas Turbine Power System", (2021).

68. Akroot, A., "Modelling of Thermal and Water Management in Automotive Polymer Electrolyte Membrane Fuel Cell Systems", ***Master Thesis***, (August): (2014).

69. Sarmah, P. and Gogoi, T. K., "Performance comparison of SOFC integrated combined power systems with three different bottoming steam turbine cycles", ***Energy Conversion And Management***, (2017).

70. Khaljani, M., Khoshbakhti Saray, R., and Bahlouli, K., "Comprehensive analysis of energy, exergy and exergo-economic of cogeneration of heat and power in a combined gas turbine and organic Rankine cycle", ***Energy Conversion And Management***, 97: 154–165 (2015).

71. Abudu, K., Igie, U., Roumeliotis, I., and Hamilton, R., "Impact of gas turbine flexibility improvements on combined cycle gas turbine performance", ***Applied Thermal Engineering***, 189: 116703 (2021).

72. Korlu, M., Pirkandi, J., and Maroufi, A., "Thermodynamic analysis of a gas turbine cycle equipped with a non-ideal adiabatic model for a double acting Stirling engine", ***Energy Conversion And Management***, 147: 120–134 (2017).

73. Akroot, A., Namli, L., and Ozcan, H., "Compared Thermal Modeling of Anode- and Electrolyte-Supported SOFC-Gas Turbine Hybrid Systems", ***Journal Of Electrochemical Energy Conversion And Storage***, (2021).

74. Akroot, A., "Effect of Operating Temperatures on the Performance of a SOFCGT Hybrid System", ***International Journal Of Trend In Scientific Research And***

Development, Volume-3 (Issue-3): 1512–1515 (2019).

75. Mendeleev, D. I., Maryin, G. E., and Akhmetshin, A. R., "Improving the efficiency of combined-cycle plant by cooling incoming air using absorption refrigerating machine", ***IOP Conference Series: Materials Science And Engineering***, 643 (1): (2019).

76. Liu, Z. and Karimi, I. A., "Simulating combined cycle gas turbine power plants in Aspen HYSYS", ***Energy Conversion And Management***, 171: 1213–1225 (2018).

77. Liu, Z. and Karimi, I. A., "New operating strategy for a combined cycle gas turbine power plant", ***Energy Conversion And Management***, 171: 1675–1684 (2018).

78. Zhong, Z., Huo, Z., Wang, X., Liu, F., and Pan, Y., "New steam turbine operational mode for a gas turbine combine cycle bottoming cycle system", ***Applied Thermal Engineering***, 198: 117451 (2021).

79. Köse, Ö., Koç, Y., and Yağlı, H., "Performance improvement of the bottoming steam Rankine cycle (SRC) and organic Rankine cycle (ORC) systems for a triple combined system using gas turbine (GT) as topping cycle", ***Energy Conversion And Management***, 211: 112745 (2020).

80. Cao, Y., Zoghi, M., Habibi, H., and Raise, A., "Waste heat recovery of a combined solid oxide fuel cell - gas turbine system for multi-generation purposes", ***Applied Thermal Engineering***, 198: 117463 (2021).

81. Li, X., Gui, D., Zhao, Z., Li, X., Wu, X., Hua, Y., Guo, P., and Zhong, H., "Operation optimization of electrical-heating integrated energy system based on concentrating solar power plant hybridized with combined heat and power plant", ***Journal Of Cleaner Production***, 289: 125712 (2021).

82. Nourpour, M. and Khoshgoftar Manesh, M. H., "Evaluation of novel integrated combined cycle based on gas turbine-SOFC-geothermal-steam and organic Rankine cycles for gas turbo compressor station", ***Energy Conversion And Management***, 252 (January): 115050 (2022).

83. Javidmehr, M., Joda, F., and Mohammadi, A., "Thermodynamic and economic analyses and optimization of a multi-generation system composed by a compressed air storage, solar dish collector, micro gas turbine, organic Rankine cycle, and desalination system", ***Energy Conversion And Management***, 168 (September 2017): 467–481 (2018).

RESUME

Alaa Fadhil KAREEM is a mechanical engineer who graduated from the Faculty of Engineering, University of Technology - Iraq. She received her Bachelor's degree in 2003. She is currently studying for her Master degree at Karabük University in the field of Mechanical Engineering.